NEMESIS
Negative Effects in Medical Sciences Oral and Maxillofacial Surgery
UCL PRESSES UNIVERSITAIRES DE LOUVAIN

Roadmap for daily practice of CBCT in cleft lip palate paediatric patients: a pictorial review.

Authors:
Olszewski R DDS, MD, PhD, DrSc, Prof[1,2*],
De Muylder A MD, DDS[1],
Siciliano S MD, DDS[3]

Affiliations:

[1] Department of oral and maxillofacial surgery, Cliniques universitaires Saint Luc, UCLouvain, Brussels, Belgium
[2] Oral and maxillofacial surgery research Lab (OMFS Lab), NMSK, IREC, UCLouvain, Brussels, Belgium
[3] Department of oral and maxillofacial surgery, Clinique Sainte Elisabeth, Brussels, Belgium
*Corresponding author: Prof Raphael Olszewski, Department of oral and maxillofacial surgery, Cliniques universitaires Saint Luc, UCLouvain, Av. Hippocrate 10, 1200 Brussels, Belgium, email: Raphael.olszewski@saintluc.uclouvain.be ORCID ID: orcid.org/0000-0002-2211-7731
Disclaimer: the views expressed in the submitted article are our own and not an official position of the institution or funder.

Abstract

Objective: to present and to illustrate a new methodology for daily practice in cone beam computed tomography (CBCT) interpretation and reporting in cleft lip palate (CLP) non syndromic paediatric patients. The proposed protocol is based on clinical experience and on systematic search of the literature.

Material and methods: We performed two types of systematic search of articles: 1) articles related to the use of CBCT in CLP patients, and 2) articles related to the reporting and interpretation of the CBCT images by radiologists. We used two databases PubMed and Google scholar.

Results: For indications of CBCT in CLP patients we found in PubMed 378 articles and 48 articles were selected for the review; in Google scholar we found 463 articles, and 9 articles were selected for the review. 2) For reporting in CBCT we found 956 articles in PubMed, and 9 articles were selected for the review.

Conclusions: We presented the 6-steps system for interpretation and reporting information from CBCT of CLP paediatric patients: 1) Step 1 (axial view): presence or absence of bone bridge remnants of alveolar bone graft; Step 2 (3D dental tissue reconstruction): description of dental arch tooth by tooth, search for agenesis and supernumerary teeth, description of variation in the position of the tooth explaining the type of existing translation and rotation; Step 3 (coronal view): cleft palate pathway and its extension; anomaly in maxillary, ethmoid and sphenoid sinuses if existing; Step 4 (sagittal and coronal view): checking of the opening (calcification sites) of the sphenooccipital synchondrosis, and checking of anomalies of the occipital bone; Step 5 (3D bone tissue reconstruction): C1-C2 vertebra anomalies; Step 6 (3D soft tissue reconstruction): external ear anomalies. We illustrated our methodology with 46 figures from 5 CBCT of CLP patients.

Keywords: cone beam computed tomography, CBCT, cleft lip palate, paediatric, reporting

Introduction

The main indication of using cone beam computed tomography (CBCT) in paediatric dentistry is related to cleft palate and cleft lip palate (CLP) patients [1, 2]. The CBCT was mainly used in CLP patients to study the secondary alveolar bone grafting [3- 29]. CBCT was also used to evaluate maxillary expansion in CLP patients [6, 30-36]. Moreover, CBCT was also used in various anatomical studies related with CLP patients: 1) Three-dimensional (3D) analysis of craniofacial structures [3, 29, 37], and of facial asymmetry [29, 38, 39]; 2) mandible [3, 29, 40, 41]; 3) sella turcica [42]; 4) pharyngeal airway volume [3, 43-48]; 5) cortical bone thickness around the cleft area [26, 27, 29, 49]; 6) palatal morphology and soft tissue depth [6, 28, 29, 50, 51]; 7) maxillary sinus volume [29, 52, 53]; 8) nasal morphology [3, 29, 54], and nasal airway [55]; 9) canine eruption through the alveolar graft bone [3, 4, 6, 7, 27, 56, 57]; 10) quantity, and morphological variation of teeth present around the cleft [3, 5-7, 27, 29, 57]; 11) cervical vertebrae [58]. However, all of these studies do not give guidance in reporting information from CLP CBCT examinations.

Limited guidelines for reporting CBCT dataset were already proposed in endodontics [59-61], implantology [59, 60], periodontology [60], lower third molars [60], and in orthodontics [60, 62]. There exists an agreement between authors that all the field of view must be viewed and described when reporting CBCT images [57, 59, 60, 63, 64].

However, Miles et al. reported that 98% of medical radiology residents received no formal training in radiology reporting [64], and 78% learned the process from a fellow resident [64]. Therefore, Miles et al. proposed to introduce a new software (Easyriter) for building structured CBCT reports including: 1) Paranasal sinuses, 2) Nasal cavity, 3). Airway, 4) Cervical structures, 5) Temporomandibular joints (TMJ), 6) Dental findings, and 7) Other findings [64]. Kachlan et al., described structured CBCT reports for incidental findings in craniomaxillofacial and cervical area: 1) Jaws, 2) Paranasal sinus, 3) Nasal fossa, 4) Pharyngeal airway, 5) TMJ, 6) Skull base/brain, 7) Neck soft tissues, and 8) Others [65].

Only two articles were related to the reporting of CBCT findings in CLP patients [66, 67].

Santos et al. described incidental findings in CLP patients situated in the following areas: 1) Skull, 2) Paranasal sinuses, 3) Orbit, 4) Middle and inner ear cavity, 5) Pharynx, 6) TMJ, 7) Cervical spine, 8) Maxilla, and 9) Mandible [66]. Only general information was given by the authors on CBCT image modalities used to search for incidental findings such as 3D reconstructions with varying opacities, reconstructed panoramic radiographs, and axial slices of the maxilla and mandible [66].

The authors also found anomalies in dental development including supernumerary teeth, teeth with atypical crown and/or root morphology, missing, ectopic, and impacted dentition [66]. The article by Santos et al is accessible in closed access

only (paywall). The article contains only 4 figures: one axial slice without any anomaly, and three 3D reconstruction figures without arrows showing 1) an ectopic impacted central incisor, 2) a missing lateral maxillary incisor, and 3) impacted maxillary canine.
Bezerra et al., [67] separated dental development anomalies in CLP patients into 3 categories: 1) Agenesis (second incisor, second premolar), 2) Microdontia (conical lateral incisor), and 3) Giroversion (central incisor). The article by Bezerra et al is accessible in open access (free article for readers) [67]. However, three figures show only the presence of left alveolar cleft [67]. Figures that may illustrate dental development anomalies are missing [67].
The aim for our article was to present and to illustrate a new methodology for daily practice in CBCT interpretation and reporting in CLP non syndromic paediatric patients. The proposed protocol is based on clinical experience and on systematic search of the literature.

Materials and methods

We performed two types of systematic search of articles for this review: 1) articles related to the use of CBCT in CLP patients, and 2) articles related to the reporting and interpretation of the CBCT images by radiologists.

1. Search for articles related to the use of CBCT in CLP patient

First, we systematically searched for articles related to the use of CBCT in CLP patients in PubMed and in Google Scholar. The inclusion criteria were: patients with maximal age of 13 years-old, and studies centred on the use of CBCT. The exclusion criteria were: CLP in adult patients, mixed groups with included children below and over 13-years-old, experimental studies, animal studies, studies where the age of patients was not given, and articles without abstract. The criterium of the threshold of the patient age is related to the fact that the late alveolar surgery in CLP patients is performed until the age of 13 years-old. We selected articles only in English without a limit of time. One observer performed the search. The articles were selected based on the title and abstract.
In PubMed we used the following search equations:

1. PubMed "cbct"[All Fields] AND ("cleft"[All Fields] OR "clefted"[All Fields] OR "clefting"[All Fields] OR "clefts"[All Fields]). The search was performed on 30.12.2022. We found 206 articles, and 47 articles were selected for final review [3, 6-25, 30-50, 52-56].

2. PubMed "cbct"[All Fields] AND ("cleft"[All Fields] OR "clefted"[All Fields] OR "clefting"[All Fields] OR "clefts"[All Fields]) AND ("applicabilities"[All Fields]

OR "applicability"[All Fields] OR "application"[All Fields] OR "applications"[All Fields] OR "applicative"[All Fields]). The search was performed on 30.12.2022. We found 20 articles, and 1 article was selected for final review [1].

3. PubMed "cbct"[All Fields] AND ("cleft"[All Fields] OR "clefted"[All Fields] OR "clefting"[All Fields] OR "clefts"[All Fields]) AND ("evaluability"[All Fields] OR "evaluate"[All Fields] OR "evaluated"[All Fields] OR "evaluates"[All Fields] OR "evaluating"[All Fields] OR "evaluation"[All Fields] OR "evaluation s"[All Fields] OR "evaluations"[All Fields] OR "evaluative"[All Fields] OR "evaluatively"[All Fields] OR "evaluatives"[All Fields] OR "evaluator"[All Fields] OR "evaluator s"[All Fields] OR "evaluators"[All Fields]). The search was performed on 30.12.2022. We found 132 articles, and no articles were selected.

4. PubMed "cbct"[All Fields] AND ("protocol"[All Fields] OR "protocol s"[All Fields] OR "protocolized"[All Fields] OR "protocols"[All Fields]) AND ("cleft"[All Fields] OR "clefted"[All Fields] OR "clefting"[All Fields] OR "clefts"[All Fields]). The search was performed on 30.12.2022. We found 20 articles, and no articles were selected.

In Pubmed we found 378 articles and 48 articles were finally selected for the review [1, 3, 6-25, 30-50, 52-56].
In Google Scholar we used the following search equation: "children with cleft lip and palate CBCT 3D". The search was performed on 30.12.2022. We found 463 articles, and 9 articles were finally selected after full text lecture [2, 4, 5, 26-28, 51, 57, 58].

2. Search for articles related to the reporting and interpretation of the images by radiologists

We used only PubMed database. The selected articles were only in English. The inclusion criteria were the articles with abstract, the articles related to the reporting CBCT examinations in dentistry (including orthodontics) and in maxillofacial surgery.
In PubMed we used the 4 following search equations:

1. PubMed: "interpretation CBCT"
("interpret"[All Fields] OR "interpretability"[All Fields] OR "interpretable"[All Fields] OR "interpretating"[All Fields] OR "interpretation"[All Fields] OR "interpretation s"[All Fields] OR "interpretational"[All Fields] OR "interpretations"[All Fields] OR "interpretative"[All Fields] OR "interpreted"[All Fields] OR "interpreter"[All Fields] OR "interpreter s"[All Fields] OR "interpreters"[All Fields] OR "interpreting"[All Fields] OR "interpretive"[All Fields] OR "interpretively"[All Fields] OR "interprets"[All Fields]) AND "CBCT"[All Fields]

Translations interpretation: "interpret"[All Fields] OR "interpretability"[All Fields] OR "interpretable"[All Fields] OR "interpretating"[All Fields] OR "interpretation"[All Fields] OR "interpretation's"[All Fields] OR "interpretational"[All Fields] OR "interpretations"[All Fields] OR "interpretative"[All Fields] OR "interpreted"[All Fields] OR "interpreter"[All Fields] OR "interpreter's"[All Fields] OR "interpreters"[All Fields] OR "interpreting"[All Fields] OR "interpretive"[All Fields] OR "interpretively"[All Fields] OR "interprets"[All Fields]
We performed this search on 26.11.2022. We found 755 articles, and 6 articles were selected after full lecture of articles [59, 60, 62-65].

2. PubMed: "CBCT reporting guidelines"
"CBCT"[All Fields] AND ("reportable"[All Fields] OR "reporting"[All Fields] OR "reportings"[All Fields] OR "research report"[MeSH Terms] OR ("research"[All Fields] AND "report"[All Fields]) OR "research report"[All Fields] OR "report"[All Fields] OR "reported"[All Fields] OR "reports"[All Fields]) AND ("guideline"[Publication Type] OR "guidelines as topic"[MeSH Terms] OR "guidelines"[All Fields])
We performed this search on 29.12.2022. We found 58 articles, and 1 article was selected [61].

3. PubMed: "reporting interpretation CBCT"
("reportable"[All Fields] OR "reporting"[All Fields] OR "reportings"[All Fields] OR "research report"[MeSH Terms] OR ("research"[All Fields] AND "report"[All Fields]) OR "research report"[All Fields] OR "report"[All Fields] OR "reported"[All Fields] OR "reports"[All Fields]) AND ("interpret"[All Fields] OR "interpretability"[All Fields] OR "interpretable"[All Fields] OR "interpretating"[All Fields] OR "interpretation"[All Fields] OR "interpretation s"[All Fields] OR "interpretational"[All Fields] OR "interpretations"[All Fields] OR "interpretative"[All Fields] OR "interpreted"[All Fields] OR "interpreter"[All Fields] OR "interpreter s"[All Fields] OR "interpreters"[All Fields] OR "interpreting"[All Fields] OR "interpretive"[All Fields] OR "interpretively"[All Fields] OR "interprets"[All Fields]) AND "CBCT"[All Fields]
We performed this search on 26/11/2022. We found 109 articles, and no articles were finally selected.

4. PubMed: "CBCT cleft reporting"
"CBCT"[All Fields] AND ("cleft"[All Fields] OR "clefted"[All Fields] OR "clefting"[All Fields] OR "clefts"[All Fields]) AND ("reportable"[All Fields] OR "reporting"[All Fields] OR "reportings"[All Fields] OR "research report"[MeSH Terms] OR ("research"[All Fields] AND "report"[All Fields]) OR "research report"[All Fields] OR "report"[All Fields] OR "reported"[All Fields] OR "reports"[All Fields])
Translations cleft: "cleft"[All Fields] OR "clefted"[All Fields] OR "clefting"[All Fields] OR "clefts"[All Fields]

Translations reporting: "reportable"[All Fields] OR "reporting"[All Fields] OR "reportings"[All Fields] OR "research report"[MeSH Terms] OR ("research"[All Fields] AND "report"[All Fields]) OR "research report"[All Fields] OR "report"[All Fields] OR "reported"[All Fields] OR "reports"[All Fields]
We performed this search on 21.12.2022. We found 34 articles, and 2 articles were finally selected after full lecture [66, 67].

Finally, 956 articles were found, and 9 articles were selected for the review on the reporting and interpretation of dentomaxillofacial CBCT [59, 60, 62-67].
The selected articles on CBCT applications in CLP were used in introduction section. The selected articles on interpretation and reporting CBCT information were used in introduction, results and in discussion section.

Results

There were 6 closed access (paywall) [59, 61, 62, 64-66], and 3 open access (free for reading) articles [60, 63, 67] among the 9 articles selected on reporting and interpretation of dentomaxillofacial CBCT.
Seven articles provided no figures on cleft palate in CBCT [59-65]. Only two articles contained some figures of CBCT CLP patients [66, 67]. One article was available in closed access [66] and contained 4 figures: one axial view without cleft, 3 figures with 3D reconstruction showing 1) ectopic central incisor, 2) missing maxillary lateral incisor, 3) impacted maxillary canine. Only one article was accessible free of charge (open access) [67] and contained three figures of left CLP (one axial view and two 3D reconstructions without arrows).
We used Planmeca Promax 3D mid CBCT with 90Kvp generator. The radiological protocol was set as following: 200µm slice thickness, 16x6.2cm (diameter x height) field of view including maxilla, skull base, C1 and C2 vertebra. We used an ultra-low dose protocol for all our patients as they were children. The acquisition time was of 6 seconds.
We used the following 6-steps system for interpretation and reporting information from CBCT of CLP paediatric patients:
Step 1. Axial view: we searched for presence or absence of bone bridge remnants of alveolar bone graft (iliac crest).
Step 2. 3D dental tissue reconstruction: we describe dental arch from tooth n°18/17 to n°28/27, we search for agenesis and supernumerary teeth, we describe each variation in the position of the tooth explaining the type of existing translation and rotation.
Step 3. Coronal view: we search for cleft palate pathway and its extension; we describe any anomaly in maxillary, ethmoid and sphenoid sinuses if existing.
Step 4. Sagittal and coronal view: we check the opening (calcification sites) of the sphenooccipital synchondrosis, and we are checking potential anomalies of the occipital bone.

Step 5. 3D bone tissue reconstruction: we search for C1-C2 vertebra anomalies.
Step 6. 3D soft tissue reconstruction: we search for external ear anomalies. In Planmeca Promax 3D mid CBCT only the right external ear is almost accessible for interpretation. The left external ear is cut at the level of the left external auditory canal.
We illustrate our 6-steps system for interpretation and reporting CBCT information in the 5 following clinical examples.

1. Patient 9 years-old, left cleft lip palate, 3 weeks postoperative control

Step 1. Axial view: we search for presence or absence of bone bridge remnants of alveolar bone graft (iliac crest).

Fig. 1. Axial view. Arrows: presence of bone bridge of alveolar bone graft between teeth n°21 and n°23.

Step 2. 3D dental tissue reconstruction: we describe the dental arch tooth by tooth.

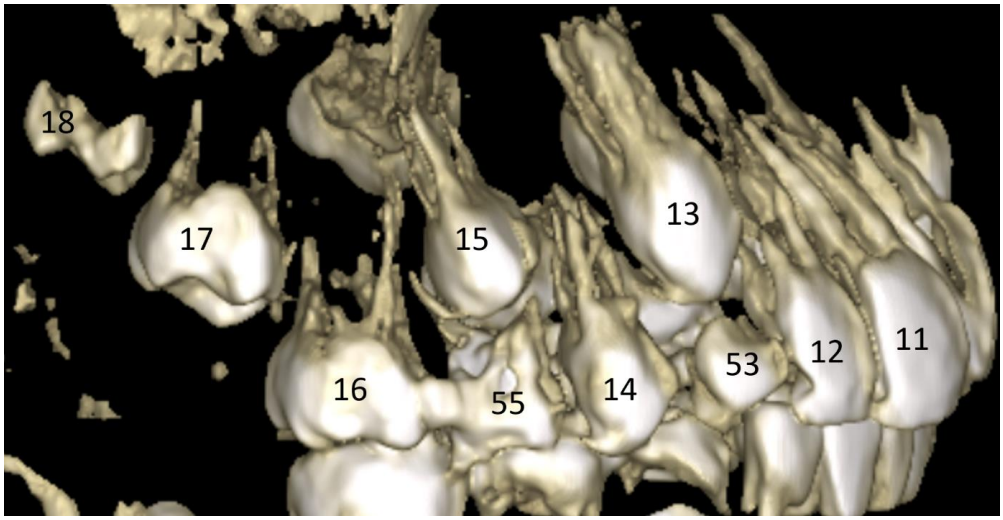

Fig. 2. 3D reconstruction. Right lateral view. Germ bud of tooth n°18 deeply non-erupted, tooth n°17 non-erupted, tooth n°16 on the arch, tooth n°55 on the arch, tooth n°15 non-erupted, with the crown surrounded by the roots of the tooth n°55, tooth n°14 on the arch, tooth n°53 on the arch, tooth n°13 vestibular and non-erupted, tooth n°12 on the arch, tooth n°11 on the arch.

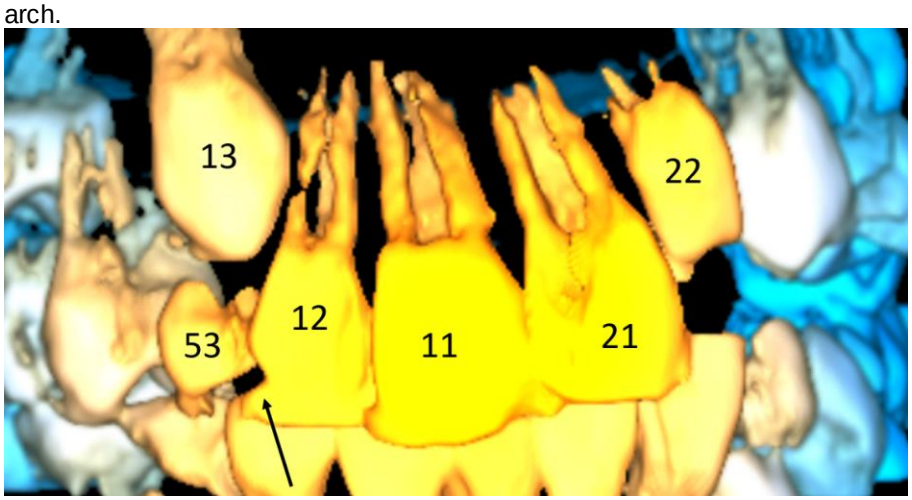

Fig. 3. 3D reconstruction. Anterior view. Tooth n°12 on the arch. There exists a malformation of the distal face of the crown (black arrow). Tooth n°11 on the arch. Tooth n°21 on the arch. Tooth n°22 impacted.

Non-erupted teeth mean that teeth are on the normal path of eruption. Impacted tooth means that the tooth is blocked in its pathway of eruption or there exists a delay in eruption relatively to the chronological age of the patient.

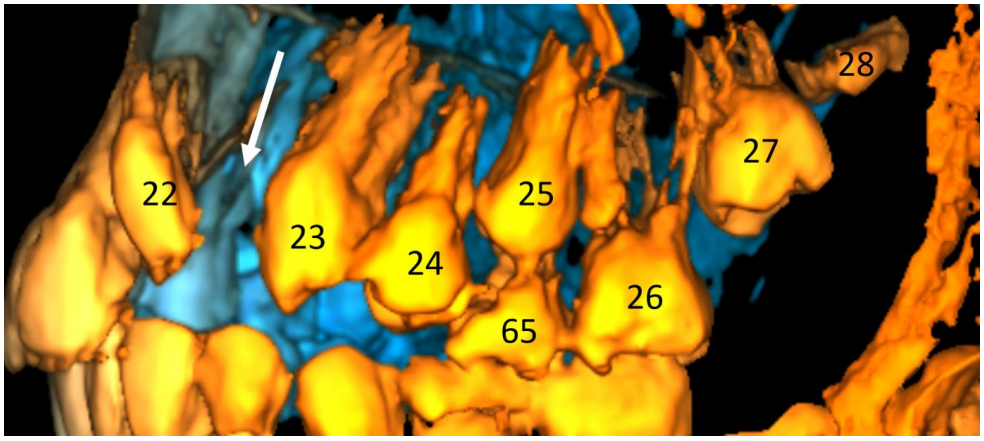

Fig. 4. 3D reconstruction. Left lateral view. Tooth n°22 impacted. The crown in oriented toward the palate in sagittal view. Tooth n°23 on the arch. Tooth n°24 on the arch. Tooth n°65 on the arch. Tooth n°25 non-erupted, with the crown surrounded by the roots of the tooth n°65. Tooth n°26 on the arch. Tooth n°27 non-erupted. Tooth n°28 deeply non-erupted. Arrow: alveolar cleft (lack of 3D reconstruction of a thin bone).

The 3D reconstruction of dental tissues does not allow to visualize alveolar bone graft and should not be used for that purpose. Only axial slices allow to evaluate the bony remnants of the alveoloplasty (Figure 1).

Step 3. Coronal view: we search for cleft palate pathway and its extension; we describe any anomaly in maxillary, ethmoid and sphenoid sinuses if existing.

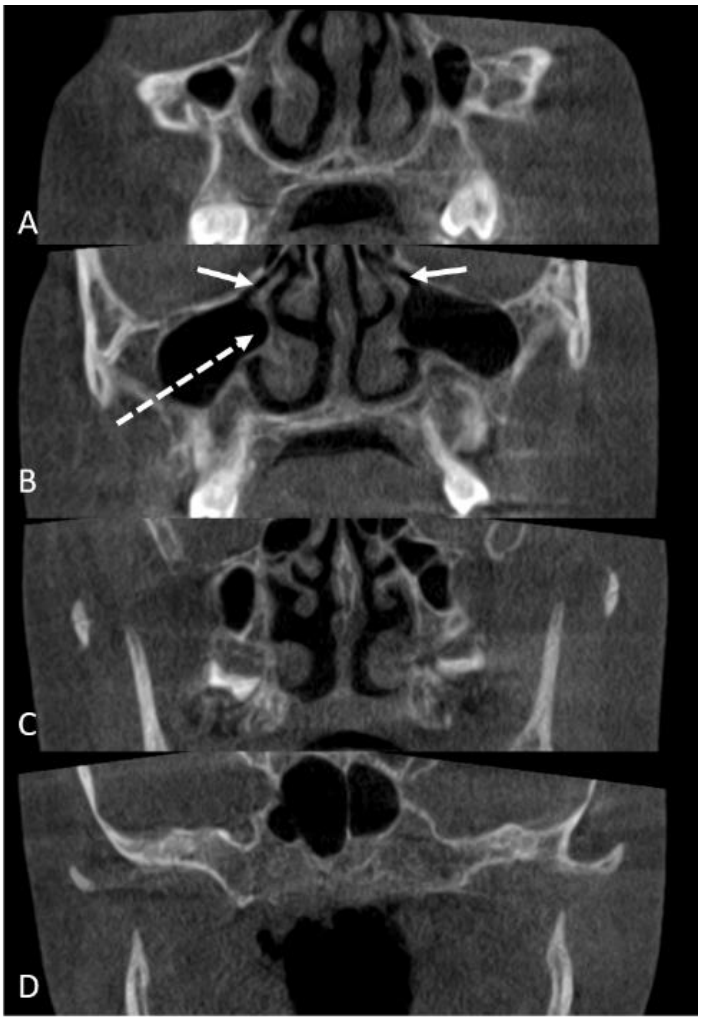

Fig. 5. 2D coronal view. A. No anomalies on the anterior view of right and left maxillary sinus. B. Area of ostium and infundibulum of right and left maxillary sinus (arrows). Pneumatisation of the root of the right inferior turbinate (dotted arrow). C. No anomalies on the posterior view of right and left maxillary sinus. D. No anomalies on the sphenoid sinus area. A-C: No presence of right/left cleft palate. A-C: No deviation of nasal septum.

Step 4. Sagittal and coronal view: we check the opening (calcification sites) of the sphenooccipital synchondrosis, and we are checking potential anomalies/variations of the occipital bone.

Fig. 6. 2D view of sphenooccipital synchondrosis. A. sagittal view. Opened sphenooccipital synchondrosis (arrows). B. Coronal view. Opened sphenooccipital synchondrosis (arrows).

Step 5. 3D bone tissue reconstruction: we search for C1-C2 vertebra anomalies. For this patient there were no anomalies related to the C1-C2 vertebra.
Step 6. 3D soft tissue reconstruction: we search for external ear anomalies.

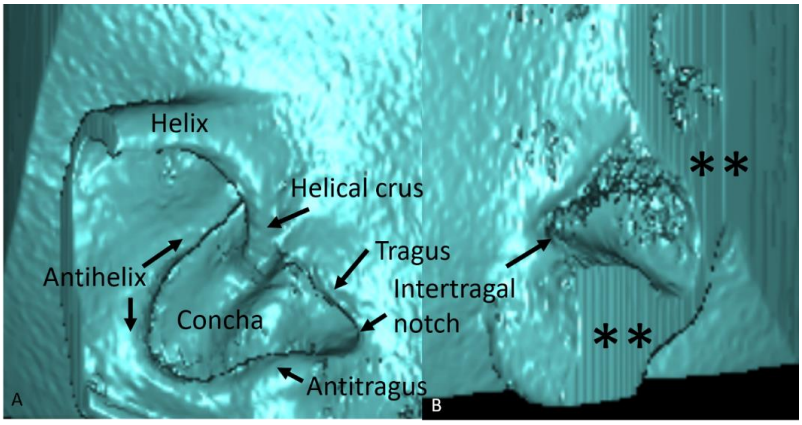

Fig. 7. 3D soft tissue external ear reconstruction. A. Right external ear. Outer part of the helix is out of the field of view. Presence of deep intertragal notch, and erasure of tragus. B. Left external ear. ** Left external ear is systematically outside the field of view.

2. Patient 7 years-old, right cleft lip palate, 6 months postoperative control

Step 1. Axial view: we search for presence or absence of bone bridge remnants of alveolar bone graft (iliac crest).

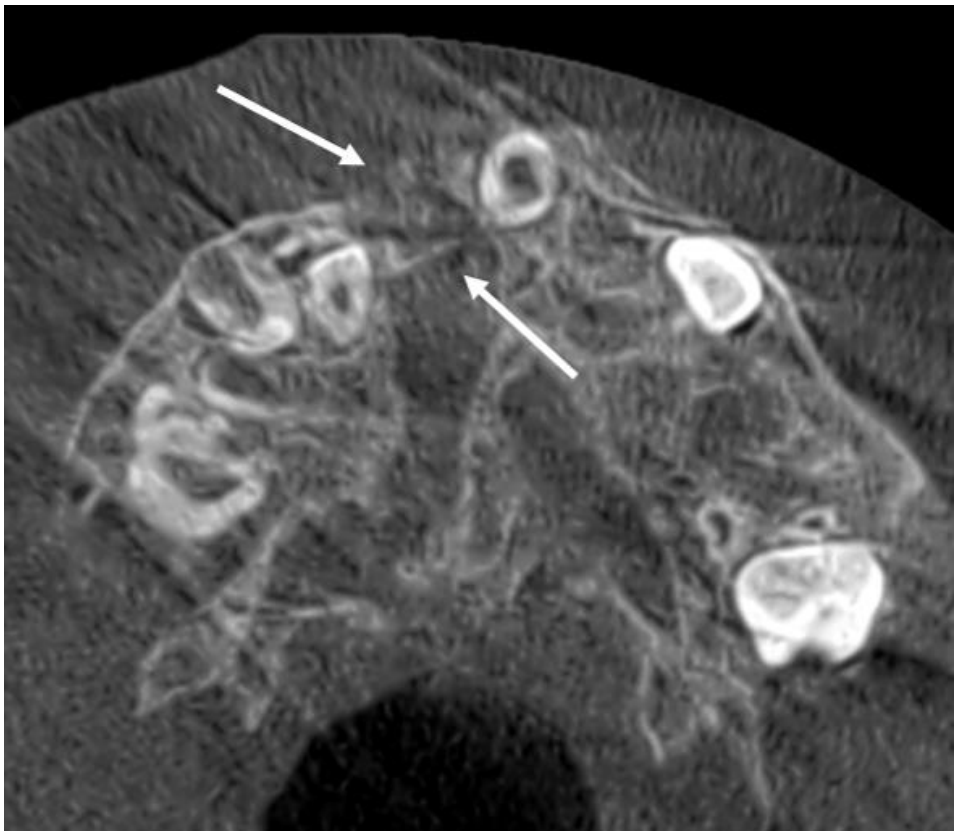

Fig. 8. Axial view. Arrows: presence of large bone bridge of alveolar bone graft between teeth n°13 and n°11.

Step 2. 3D dental tissue reconstruction: we describe the dental arch tooth by tooth.

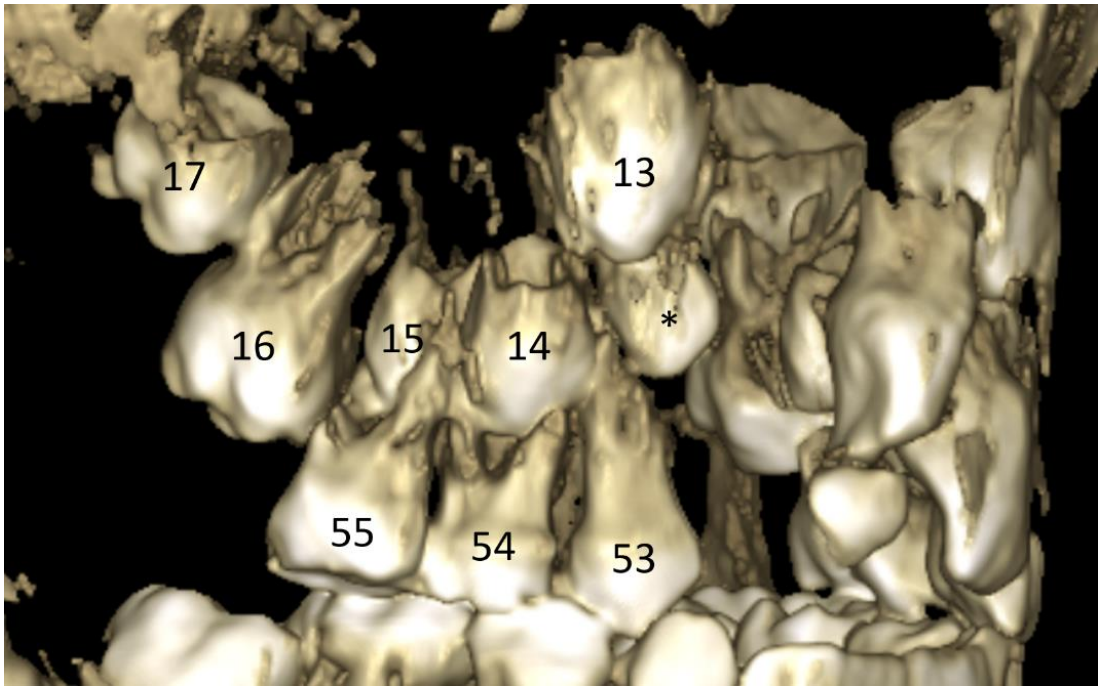

Fig. 9. 3D reconstruction. Right lateral view. Germ bud of tooth n°17 deeply non-erupted. Tooth n°16 non-erupted. Tooth n°55 on the arch. Germ bud of tooth n°15 non-erupted, surrounded by the roots of the tooth n°55, and slightly displaced to palatine side. Tooth n°54 on the arch. Germ bud of tooth n°15 non-erupted, surrounded by the roots of the tooth n°54. Tooth n°53 on the arch. *Supernumerary tooth mesial to the apex of the tooth n°53 and occlusal to the crown of the tooth n°13. Tooth n°13 non-erupted and vestibular. Agenesis of the tooth n°12. Lack of 3D reconstruction of existing alveolar bone bridge between teeth n°13 and n°11.

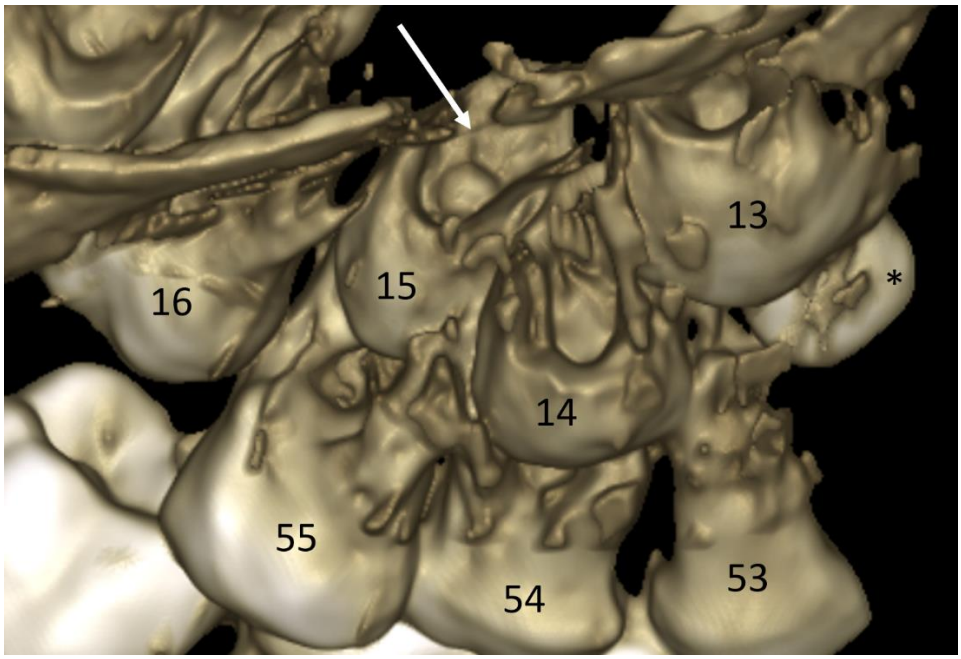

Fig. 10. 3D reconstruction. Right lateral and upper view. Germ bud of tooth n°15 non-erupted, surrounded by the roots of the tooth n°55, and slightly displaced to palatine side.

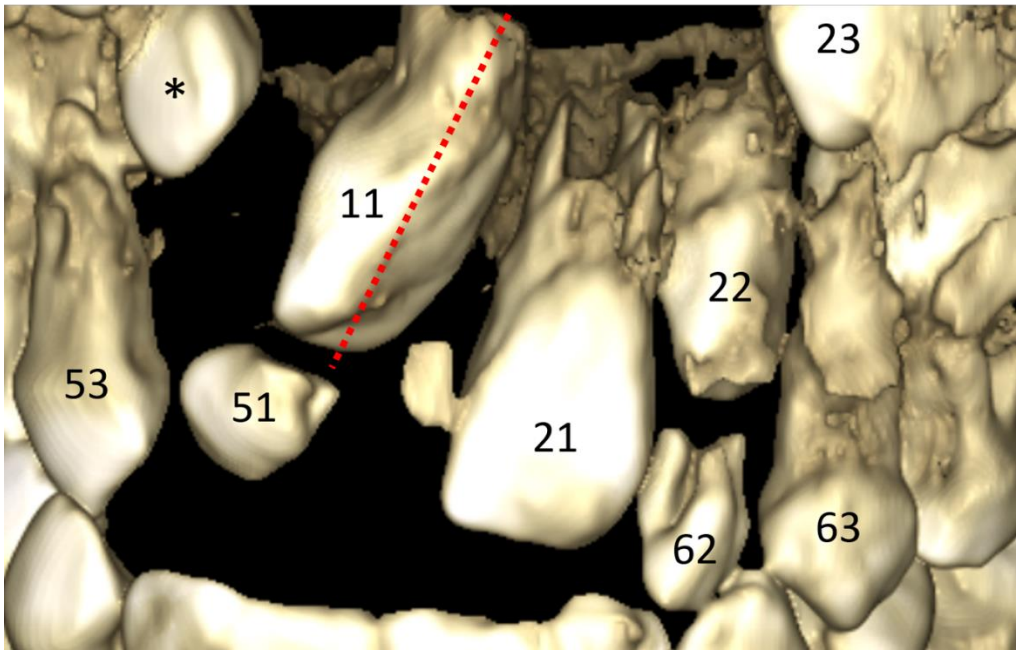

Fig. 11. 3D reconstruction. Anterior view. Tooth n°53 on the arch. *Supernumerary tooth mesial and close to the apex of the tooth n°53. Agenesis of the tooth n°12. Tooth n°51 on the arch. Toth n°11 non-erupted with rotation along its main axis (red dotted line). The distal face of the tooth n°11 is directed to the vestibular side. Tooth n°21 on the arch. Tooth n°62 on the arch. Tooth n°22 non-erupted. Tooth n°63 on the arch. Tooth n°23 non-erupted and apical to the apex of the tooth n°63.

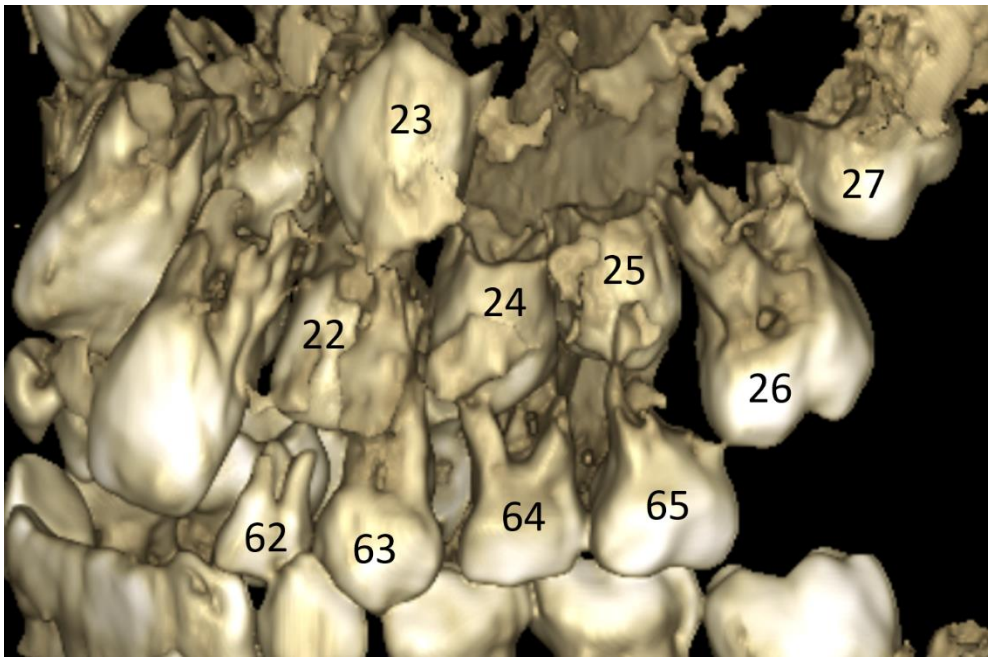

Fig. 12. 3D reconstruction. Left lateral view. Tooth n°62 on the arch. Tooth n°22 non-erupted. Tooth n°63 on the arch. Tooth n°23 non-erupted apical to the apex of the root of the tooth n°63. Tooth n°64 on the arch. Germ bud of the tooth n°24, non-erupted, slightly displaced to mesial in relation with the roots of the tooth n°64. Tooth n°65 on the arch. Germ bud of the tooth n°25, non-erupted, slightly displaced to mesial in relation with the roots of the tooth n°65. Tooth n°26 non-erupted. Tooth n°27 deeply non-erupted.

Step 3. Coronal view: we search for cleft palate pathway and its extension; we describe any anomaly in maxillary, ethmoid and sphenoid sinuses if existing.

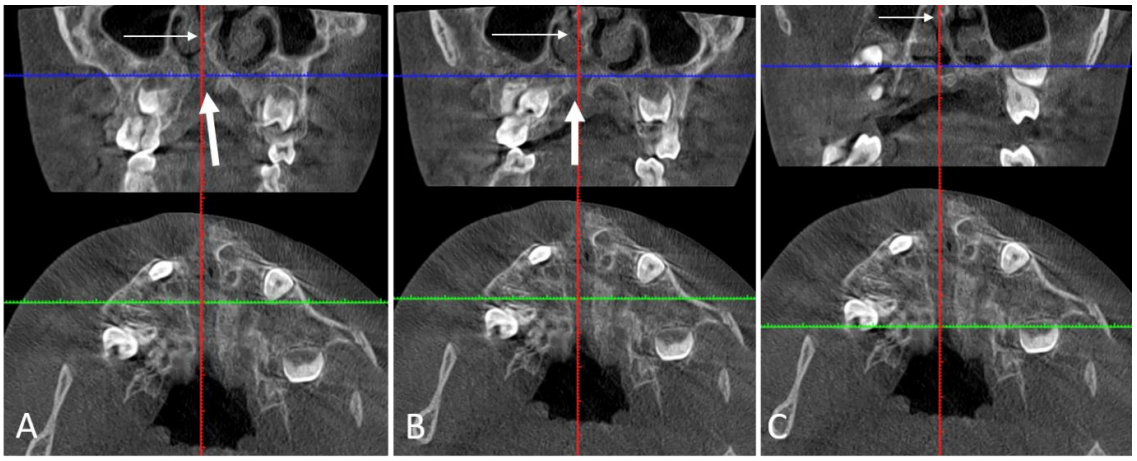

Fig. 13. Coronal (upper) and axial (lower) view. A. First premolar area. On the coronal view: thin arrow: deviation of the nasal septum to the right. Thick arrow: Right cleft palate in the area of the first premolar. B. Second premolar area. On the coronal view: thin arrow: deviation of the nasal septum to the right. Thick arrow: Right cleft palate in the area of the second premolar. C. First molar area. On the coronal view: thin arrow: deviation of the nasal septum to the right. Absence of the right cleft palate in the in the area of the first molar.

Step 4. Sagittal and coronal views: we check the opening (calcification sites) of the sphenooccipital synchondrosis, and we are checking potential anomalies/variations of the occipital bone.

Fig. 14. Sagittal view. Opened sphenooccipital synchondrosis (arrows).

Step 5. 3D bone tissue reconstruction: we search for C1-C2 vertebra anomalies.

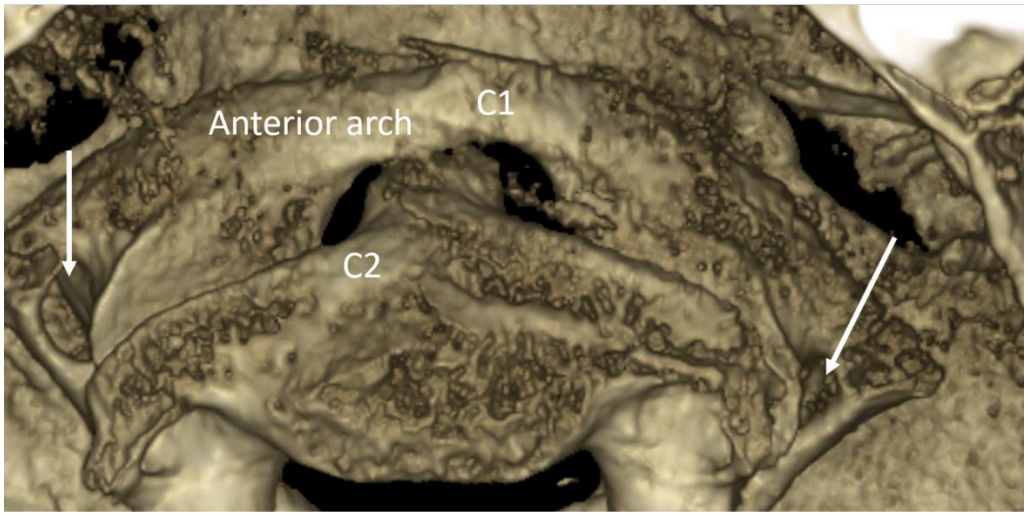

Fig. 15. 3D reconstruction of C1 and C2 vertebra. Anterior view. Normal and complete anterior arch of C1 vertebra. Arrows: Transverse foramen for right and left vertebral artery.

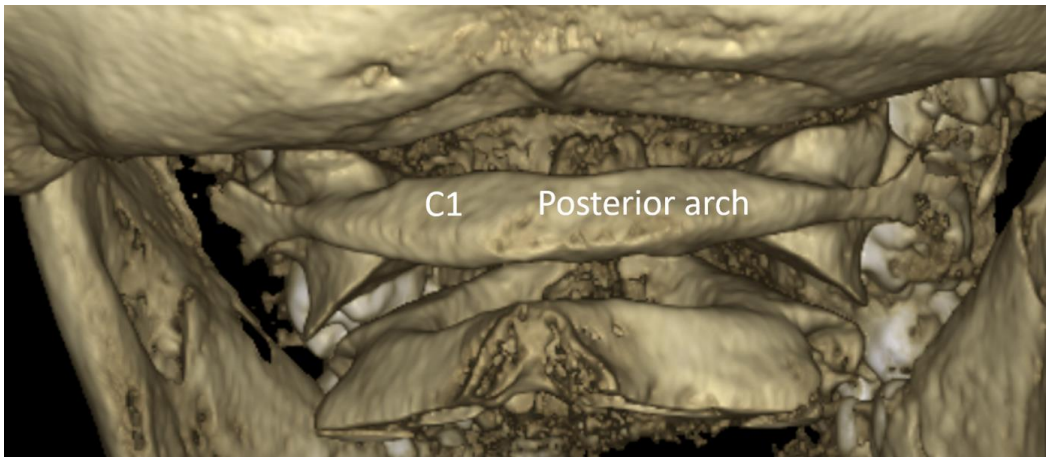

Fig. 16. 3D reconstruction of C1 and C2 vertebra. Posterior view. Normal and complete posterior arch of C1 vertebra.

Step 6. 3D soft tissue reconstruction: we search for external ear anomalies. We found no anomalies of external ears in this patient.

3. Patient 10 years-old, left cleft lip palate, 6 months postoperative control

Step 1. Axial view: we search for presence or absence of bone bridge remnants of alveolar bone graft (iliac crest).

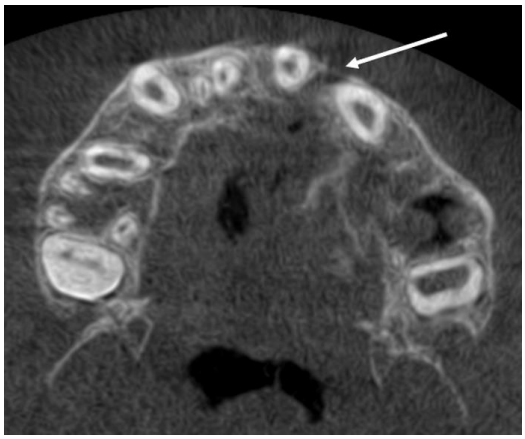

Fig. 17. Axial view. Arrow: presence of thin bone bridge of alveolar bone graft between teeth n°21 and n°23.

Step 2. 3D dental tissue reconstruction: we describe the dental arch tooth by tooth.

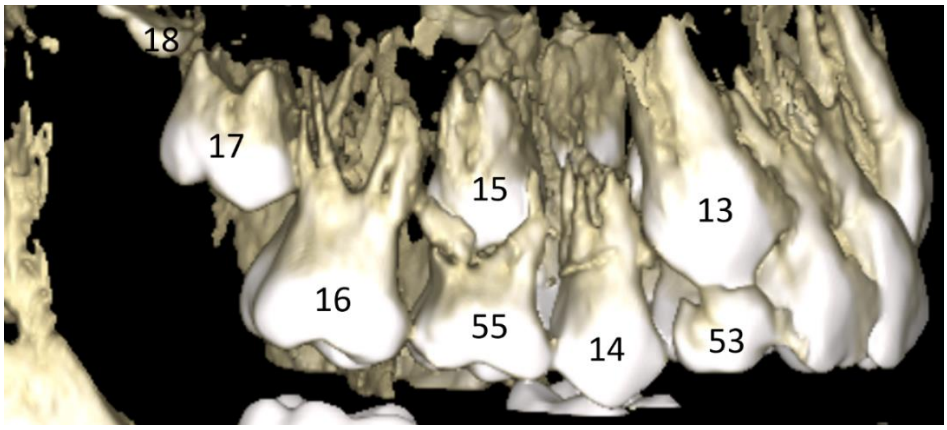

Fig. 18. 3D reconstruction. Right lateral view. Germ bud of tooth n°18 deeply non-erupted. Tooth n°17 non-erupted. Tooth n°16 on the arch. Tooth n°55 on the arch. Tooth n°15 non-erupted, and surrounded by the roots of the tooth n°55. Tooth n°14 on the arch. Tooth n°53 on the arch. Tooth n°13 non-erupted with the crown inside the tooth n°53.

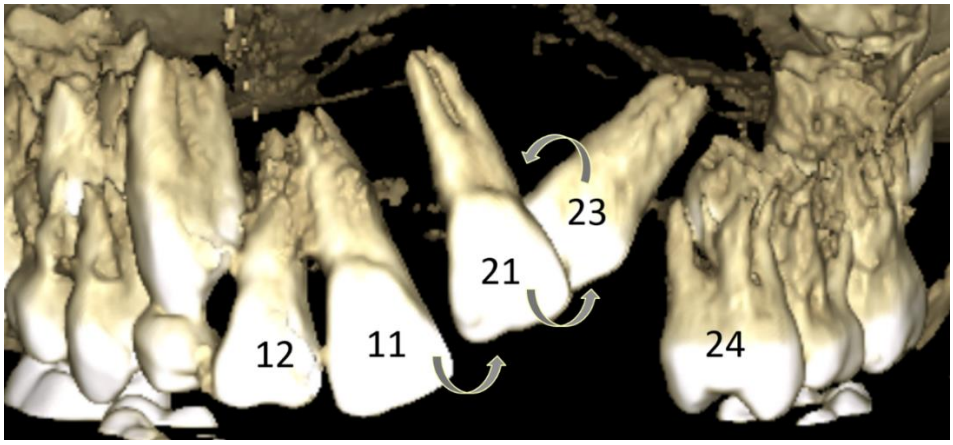

Fig. 19. 3D reconstruction. Anterior and left lateral view. Tooth n°11 tilted toward left side and toward midline (rounded arrow). Tooth n°21 tilted toward left side (rounded arrow). Agenesis of the tooth n°22. Tooth n°23 tilted toward right side (rounded arrow).

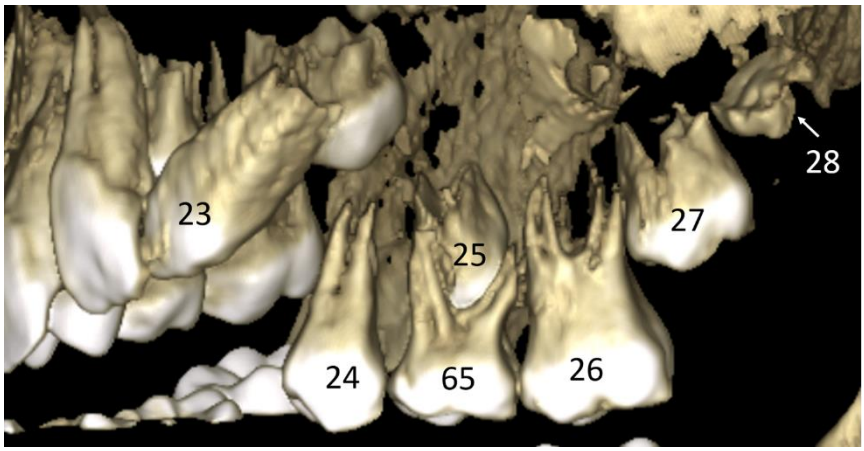

Fig. 20. 3D reconstruction. Left lateral view. Tooth n°24 on the arch. Tooth n°65 on the arch. Tooth n°25 non-erupted, and surrounded by the roots of the tooth n°65. Tooth n°26 on the arch. Tooth n°27 non-erupted. Germ bud of tooth n°28 deeply non-erupted.

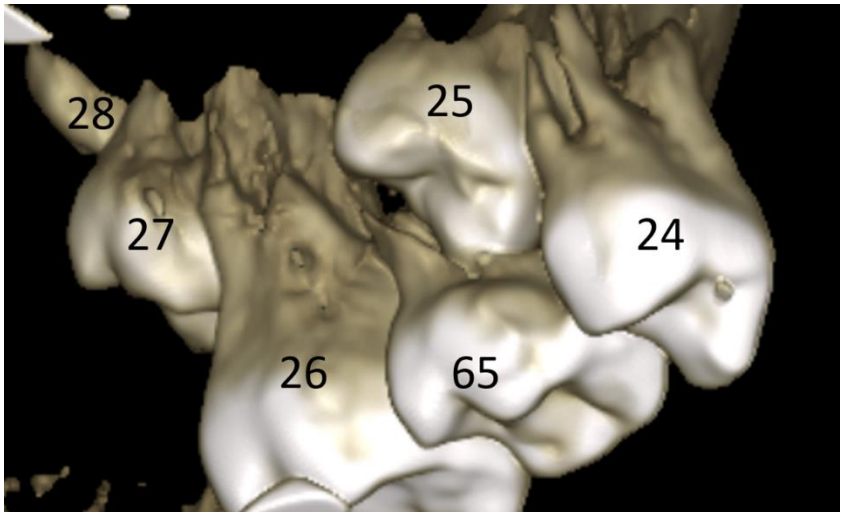

Fig. 21. 3D reconstruction. Left lateral and palatine view. Tooth n°25 displaced toward the palate.

Step 3. Coronal view: we search for cleft palate pathway and its extension; we describe any anomaly in maxillary, ethmoid and sphenoid sinuses if existing.

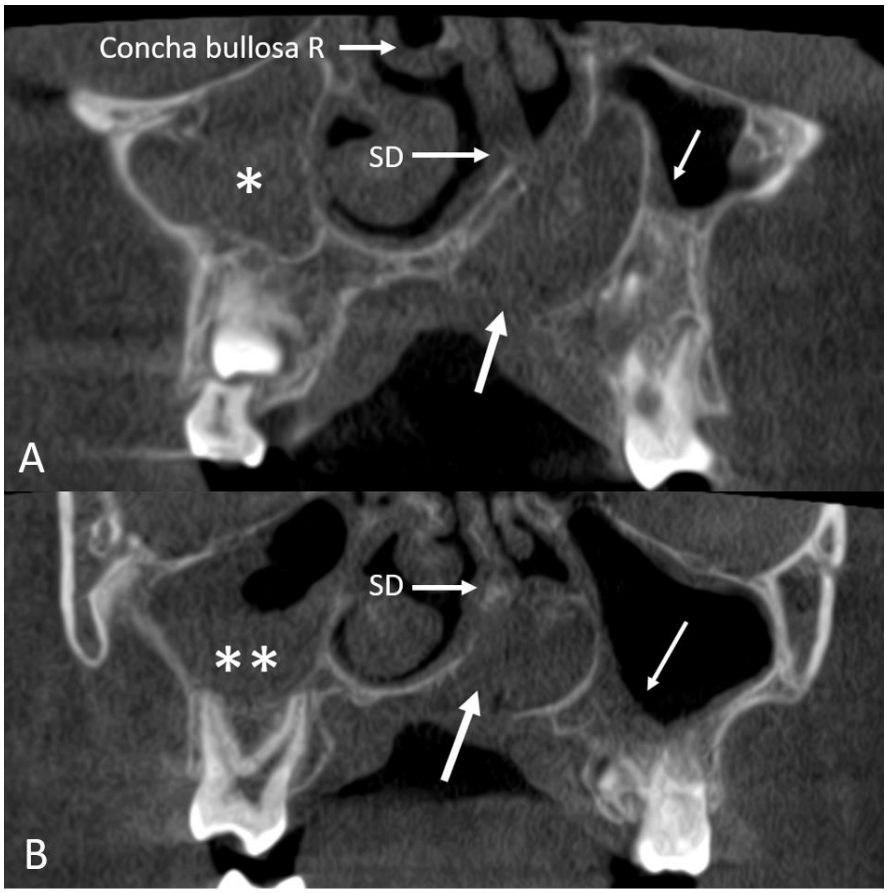

Fig. 22. Coronal view. A. Area of the tooth n°15. Cleft of the left nasal floor (thicker arrow). SD: nasal septum deviation toward left, and toward cleft palate. Right concha bullosa. * Total filling of the right maxillary sinus. Thinner arrow: thickening of the mucosa of the left maxillary sinus. B. Area of the tooth n°16. Cleft of the left nasal floor (thicker arrow). SD: nasal septum deviation toward left, and toward cleft palate. ** Important thickening of the mucosa of the right maxillary sinus. Thinner arrow: thickening of the mucosa of the left maxillary sinus.

Step 4. Sagittal and coronal view: we check the opening (calcification sites) of the sphenooccipital synchondrosis, and we check potential anomalies/variations of the occipital bone.

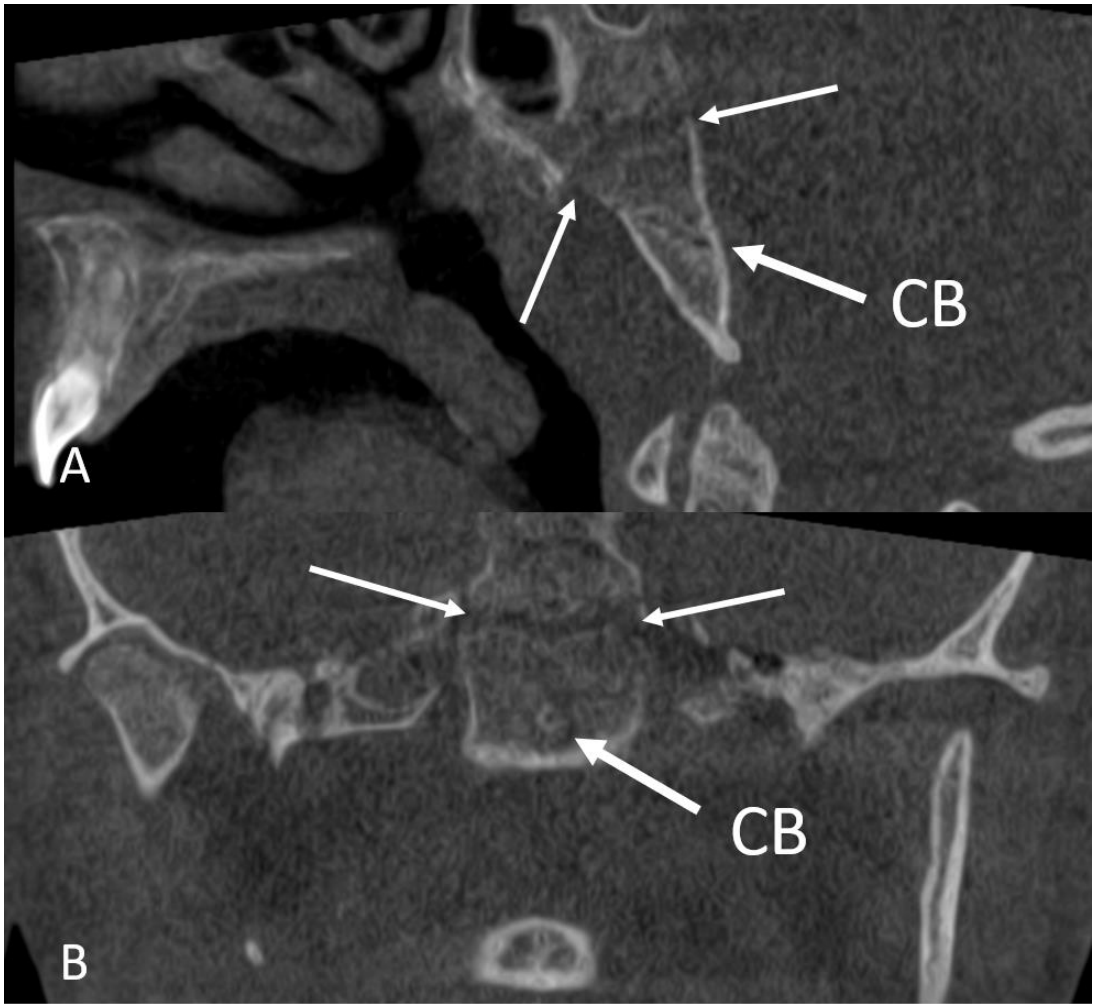

Fig. 23. A. Sagittal view. Arrows: opened sphenooccipital synchondrosis. CB: diagonal canal basilaris. B. Coronal view. Arrows: opened sphenooccipital synchondrosis. CB: unique median canal basilaris.

Step 5. 3D bone tissue reconstruction: we search for C1-C2 vertebra anomalies.

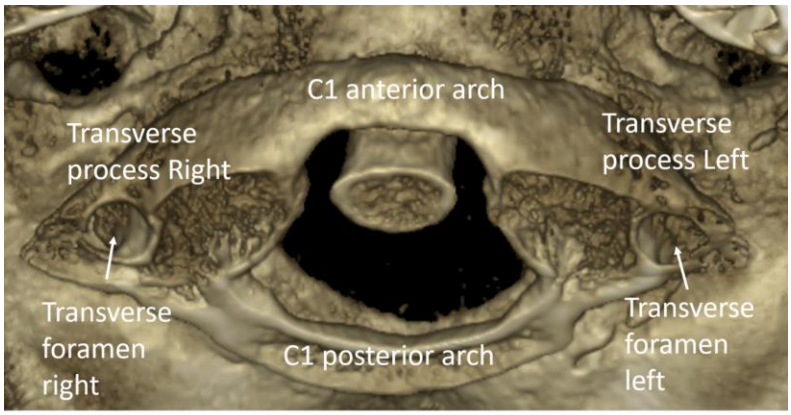

Fig. 24. 3D reconstruction of C1 vertebra. Normal anatomy of C1 vertebra. Complete anterior and posterior arch, and complete anterior and posterior walls of the transverse foramen right and left.

Step 6. 3D soft tissue reconstruction: we search for external ear anomalies. We found no anomalies of external ears in this patient.

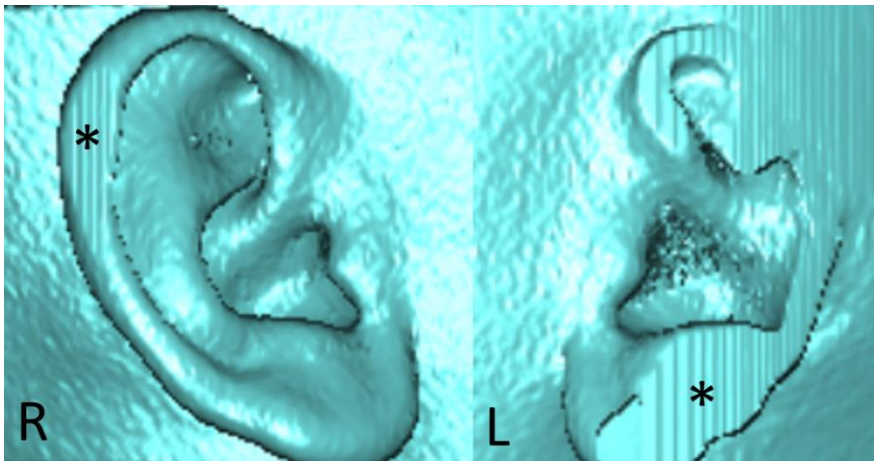

Fig. 25. 3D reconstruction of ears. R. Right ear with normal anatomy and almost complete (*area outside the field of view). L. left ear. *Major part of the left ear is situated outside of the field of view.

4. Patient 13 years-old, left cleft lip palate, evaluation of the remaining alveolar graft

Step 1. Axial view: we search for presence or absence of bone bridge remnants of alveolar bone graft (iliac crest).

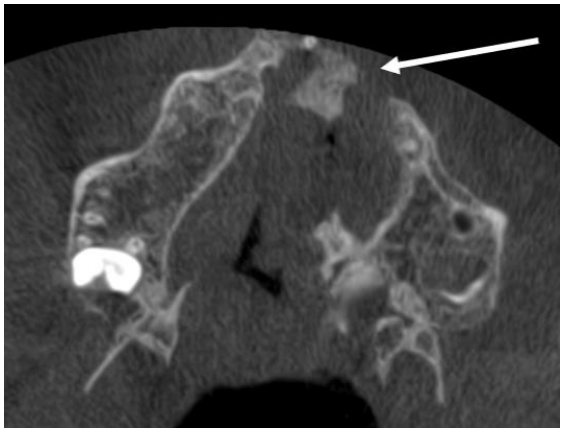

Fig. 26. Axial view. Absence of the bone wall between the fragments of the left upper maxilla (arrow).

Step 2. 3D dental tissue reconstruction: we describe the dental arch tooth by tooth.

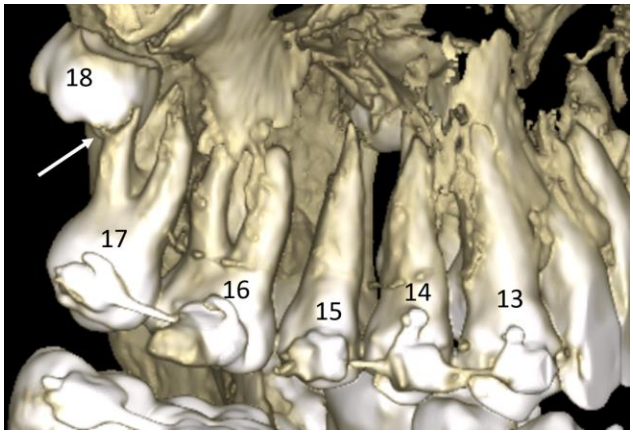

Fig. 27. 3D reconstruction. Right lateral view. Germ bud of tooth n°18 deeply non-erupted. Possible external resorption of the distovestibular root of the tooth n°17 by the tooth n°18. Tooth n°17 on the arch. Tooth n°16 on the arch. Tooth n°15 on the arch. Tooth n°14 on the arch. Tooth n°14 on the arch. Tooth n°13 on the arch.

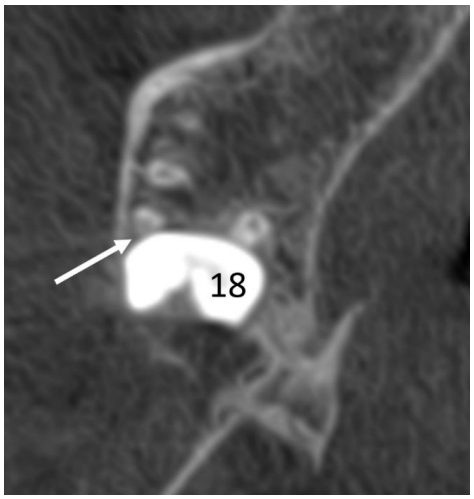

Fig. 28. Axial view. External resorption of the distovestibular root of the tooth n°17 by the tooth n°18 (arrow).

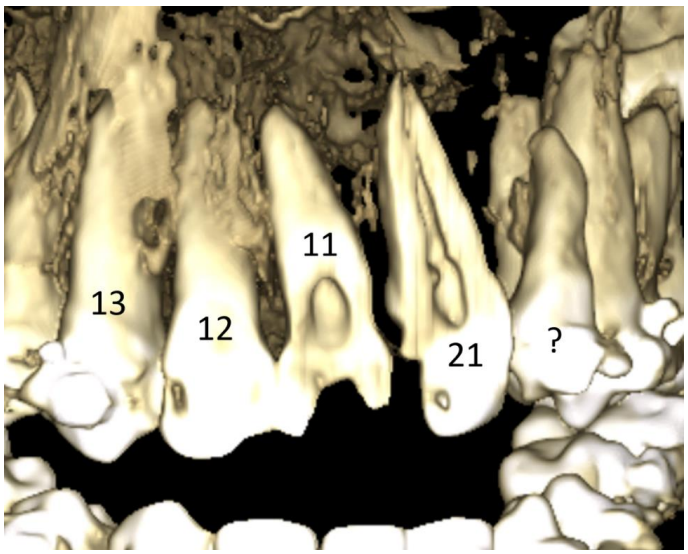

Fig. 29. 3D reconstruction. Anterior view. Tooth n°13 on the arch. Tooth n°12 on the arch. Tooth n°11 on the arch. Tooth n°21 on the arch. Slicing of the crowns and roots of teeth n°11 and 21 because the teeth are partially situated outside of the field of view. ? Need of more than one 3D reconstruction view to determine the numbering of this tooth.

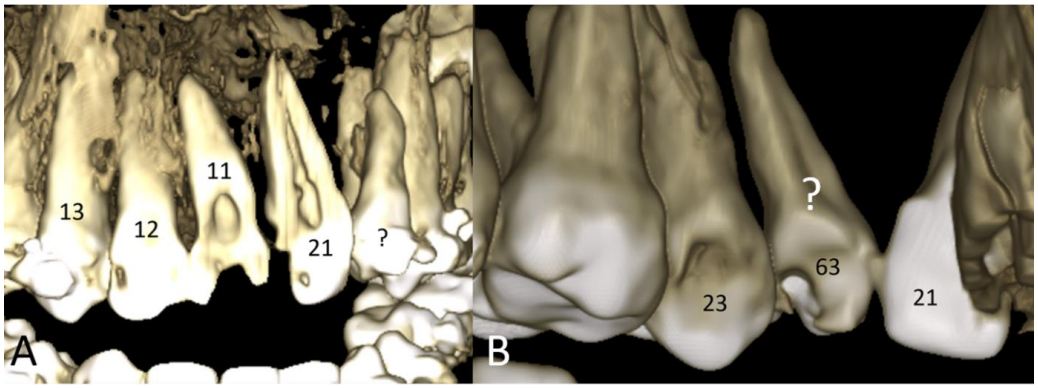

Fig. 30. A. 3D reconstruction. Anterior view. ? undetermined numbering of the tooth lateral to tooth n°21. B. 3D reconstruction. Palatine view. ? is related to the not resorbed tooth n°63 which is situated between teeth n°21 and 23.

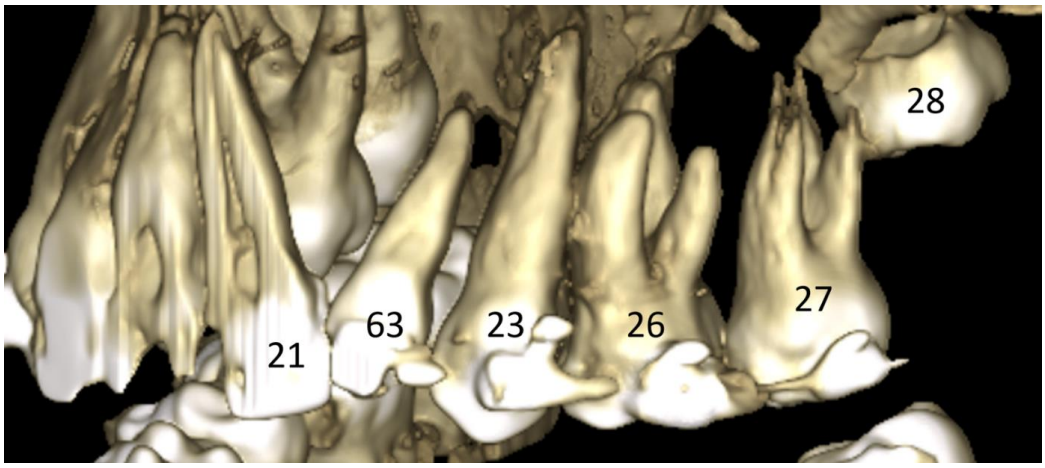

Fig. 31. 3D reconstruction. Left lateral view. Tooth n°21 on the arch. Tooth n°63 tilted to the right. Tooth n°23 on the arch and in transmigration positioned laterally to the tooth n°63. Agenesis of tooth n°24. Agenesis of the tooth n°25. Tooth n°26 on the arch. Tooth n°27 on the arch. Germ bud of tooth n°28 deeply non-erupted.

Step 3. Coronal view: we search for cleft palate pathway and its extension; we describe any anomaly in maxillary, ethmoid and sphenoid sinuses if existing.

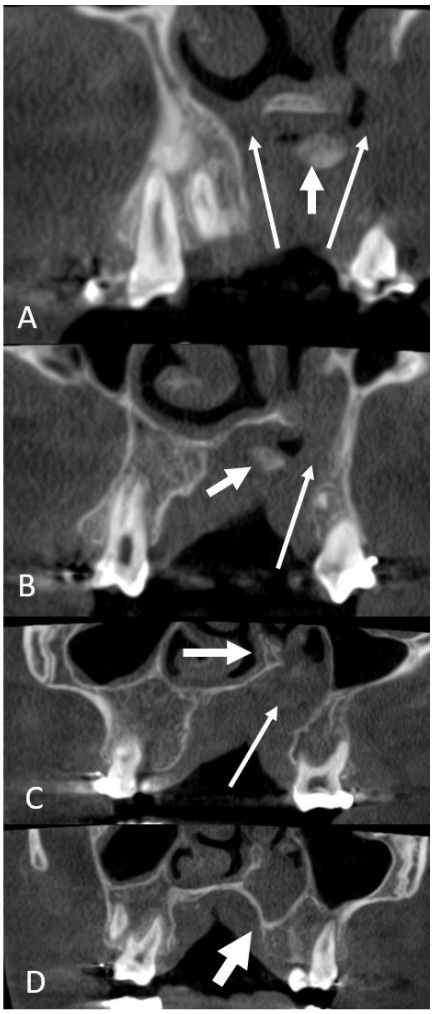

Fig. 32. Coronal view. A. Anterior area. Bilateral cleft palate (thin arrows). Remnants of the alveolar bone bridge/graft (thick arrow). B. Premolar area. Left cleft palate (thin arrow). Remnants of the alveolar bone bridge/graft (thick arrow). C. First molar area. Left cleft palate (thin arrow). Deviation of nasal septum toward left (thick arrow). D. Second molar area. No cleft palate. Left nasal fossa is deeper than the right nasal fossa (thick arrow). Right cleft palate is limited to the anterior and premolar area. Left cleft palate is extended between anterior and first molar area.

The right cleft palate is situated between the anterior and the premolar area. The left cleft palate is extended between anterior and first molar area (Figure 32).

Step 4. Sagittal and coronal view: we check the opening (calcification sites) of the sphenooccipital synchondrosis, and we check potential anomalies/variations of the occipital bone.

Fig. 33. Sagittal view. Arrows: opened sphenooccipital synchondrosis (thin arrow). Center of calcification present on the retropharyngeal side of the clivus (thick arrow).

Step 5. 3D bone tissue reconstruction: we search for C1-C2 vertebra anomalies.

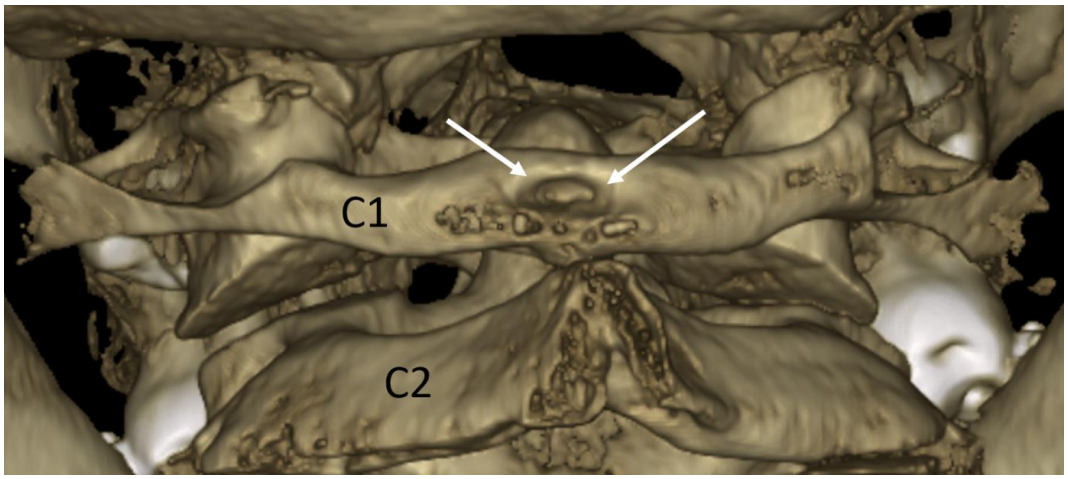

Fig. 34. 3D reconstruction. Posterior view of the C1 and C2 vertebra. Recess in the posterior arch of C1 on the midline (thin arrows).

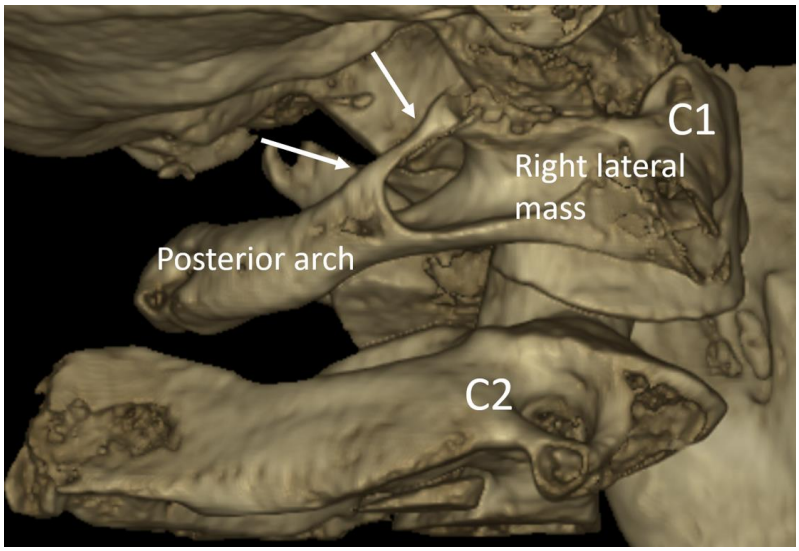

Fig. 35. 3D reconstruction. Right lateral view of C1 and C2 vertebrea. Complete ponticulus posticus (arrows) between the right lateral mass and the right posterior arch.

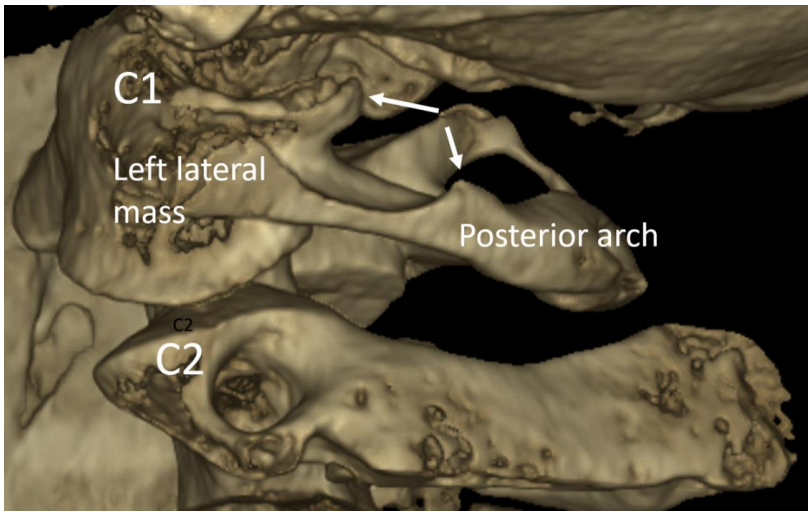

Fig. 36. 3D reconstruction. Left lateral view of C1 and C2 vertebrea. Partial ponticulus posticus (arrows) between the left lateral mass and the left posterior arch.

Step 6. 3D soft tissue reconstruction: we search for external ear anomalies. We found no anomalies of external ears in this patient.

There were no anomalies of external ears for this patient.

5. Patient 7 years-old, left cleft lip palate, evaluation before surgery

Step 1. Axial view: we search for presence or absence of bone bridge remnants of alveolar bone graft (iliac crest).

Fig. 37. Axial view. Left alveolar cleft between the fragments of the upper maxilla (arrow).

Step 2. 3D dental tissue reconstruction: we describe the dental arch tooth by tooth.

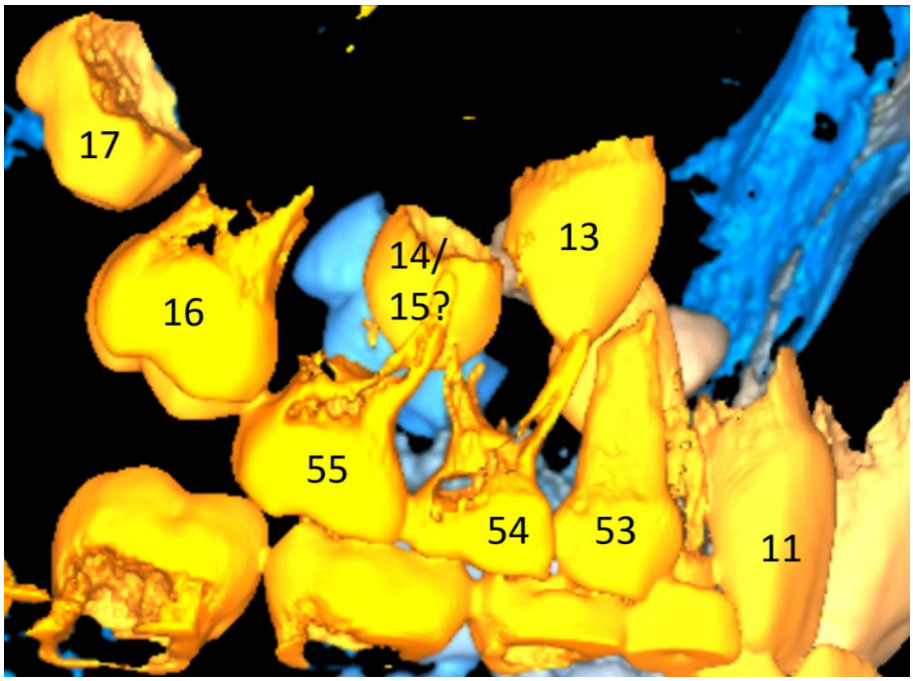

Fig. 38. 3D reconstruction. Right lateral view. Germ bud of tooth n°17 deeply non-erupted. Tooth n°16 non-erupted. Tooth n°55 on the arch. Tooth n°54 on the arch. Agenesis of the tooth n°14 or n°15, and presence of only one premolar germ bud between the mesial roots of the tooth n°55 and between the distal roots of the tooth n°54. Tooth n°53 on the arch. Tooth n°13, non-erupted, with its crown distoapical to the apex of the tooth n°53.

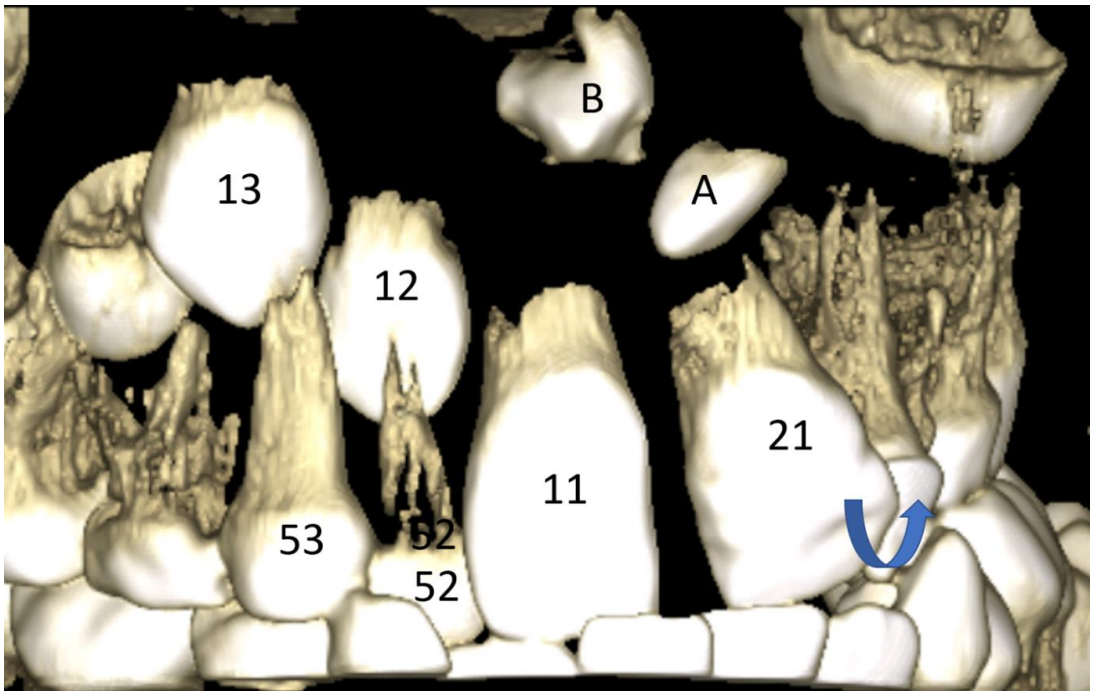

Fig. 39. 3D reconstruction. Anterior view. Tooth n°53 on the arch. Tooth n°13 non-erupted, with its crown distoapical to the apex of the tooth n°53. Tooth n°52 on the arch. Tooth n°12 non-erupted, palatine to the tooth n°52. Tooth n°11 in the arch. Tooth n°21 on the arch and tilted toward left (rounded arrow). A and B: presence of two supernumerary teeth on the left edge of the alveolar cleft.

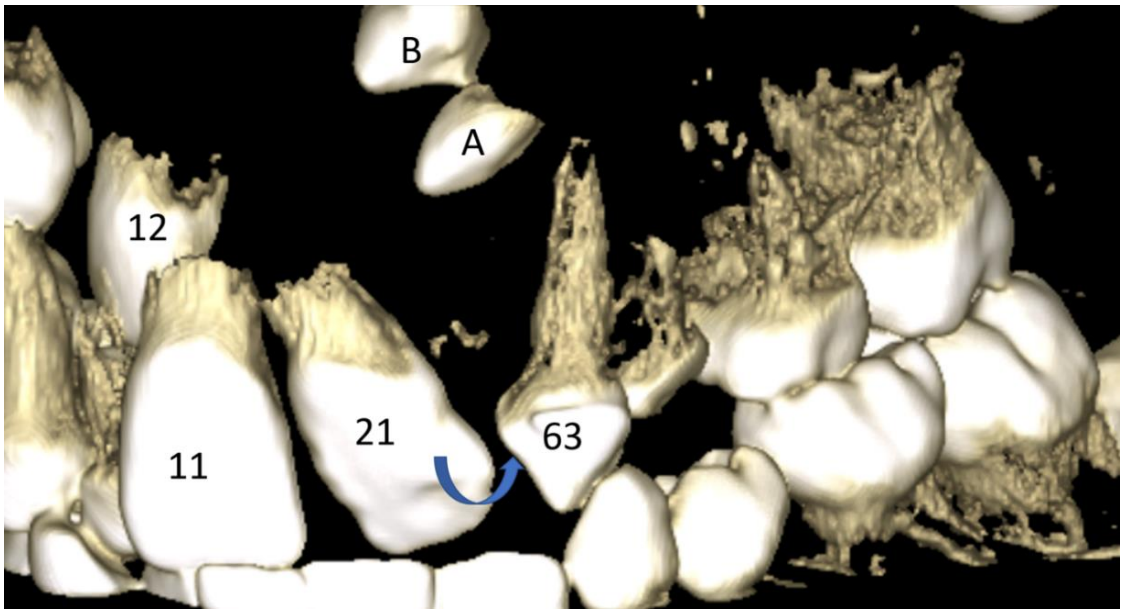

Fig. 40. 3D reconstruction. Left lateral view. Tooth n°21 on the arch, tilted toward left (rounded arrow), and rotated to the palatine side. A and B: presence of two supernumerary teeth on the left edge of the alveolar cleft. Tooth n°63 on the arch with rotation of the tooth along its main axis. The mesial side of the tooth is rotate toward vestibular side. Agenesis of teeth n°22 and 23.

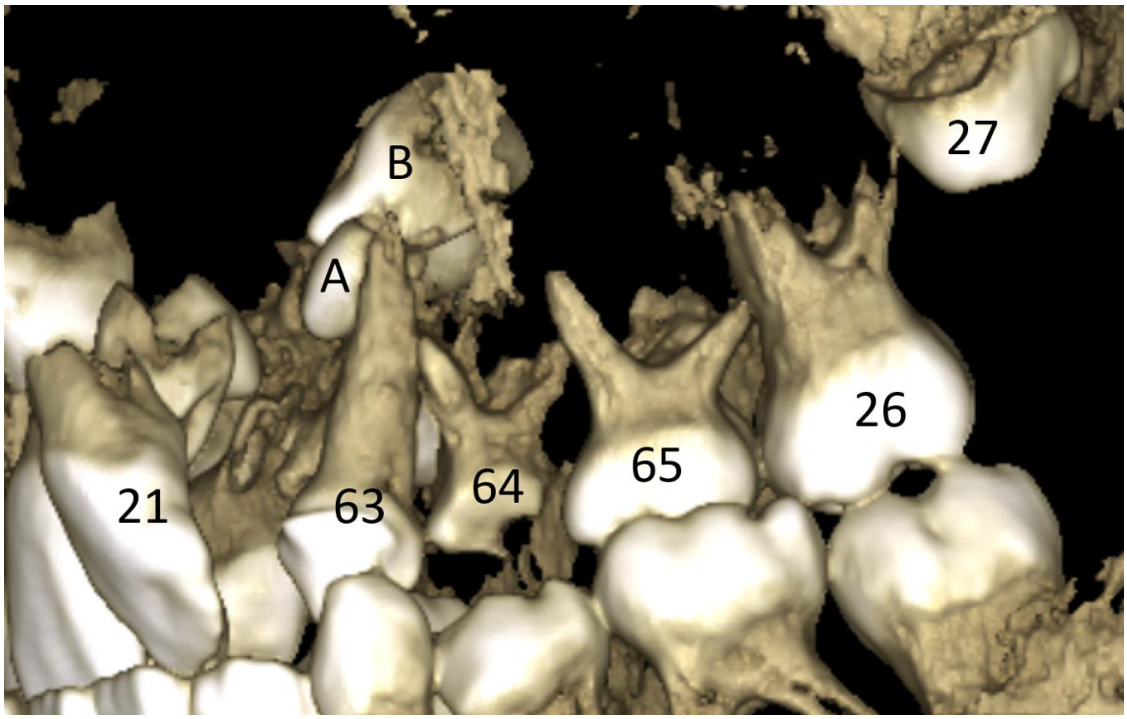

Fig. 41. 3D reconstruction. Left lateral view. A and B: presence of two supernumerary teeth on the left edge of the alveolar cleft. Tooth n°63 on the arch. Tooth n°64 on the arch. Agenesis of the tooth n°24. Tooth n°65 on the arch. Agenesis of the tooth n°25. Tooth n°26 on the arch. Germ bud of the tooth n°27 deeply non-erupted.

Step 3. Coronal view: we search for cleft palate pathway and its extension; we describe any anomaly in maxillary, ethmoid and sphenoid sinuses if existing.

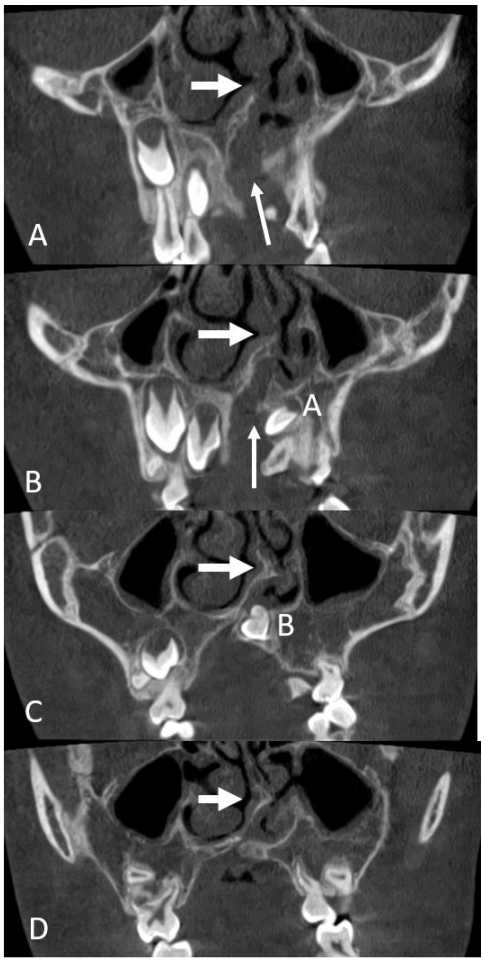

Fig. 42. Coronal view. A. Anterior area. Thin arrow: left cleft palate. Thick arrow: nasal septum deviation toward left. B. Canine area. Thin arrow: left cleft palate narrower than in the anterior area. A: presence of the supernumerary tooth A on the left edge of the cleft palate. Thick arrow: nasal septum deviation toward left. C. Premolar area. Thick arrow: nasal septum deviation toward left with the presence of the bone spur directed toward left. B: presence of the supernumerary geminated tooth A on the left edge of the cleft palate. Cleft palate is closed at this level. D. Thick arrow: nasal septum deviation toward left with the presence of the bone spur directed toward left. No cleft palate at this level.

Step 4. Sagittal and coronal view: we check the opening (calcification sites) of the sphenooccipital synchondrosis, and we check potential anomalies/variations of the occipital bone.

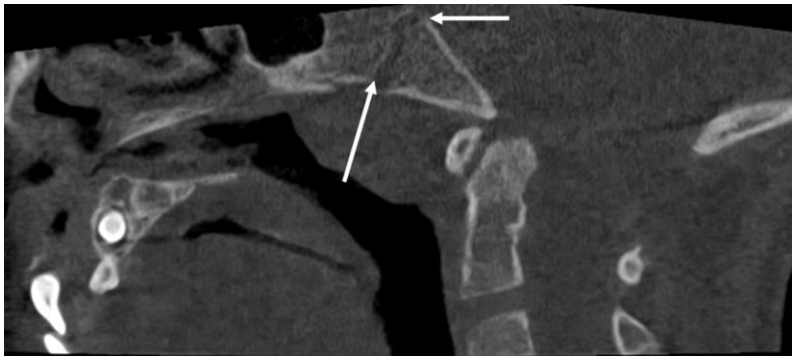

Fig. 43. Sagittal view. Arrows: opened sphenooccipital synchondrosis (thin arrow).

Step 5. 3D bone tissue reconstruction: we search for C1-C2 vertebra anomalies.

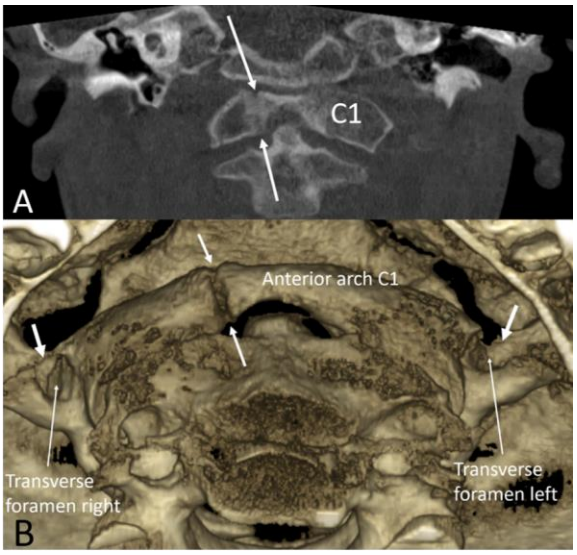

Fig. 44. A. Coronal view. Arrows: non fusion of the right neurocentral synchondrosis on the anterior arch (normal fusion at the age of 6 years-old). B. 3D reconstruction. Anterior view of the C1 vertebra. Arrows: non fusion of the right neurocentral synchondrosis on the anterior arch. Thicker arrows: absence of the anterior wall of the transverse foramen (right and left).

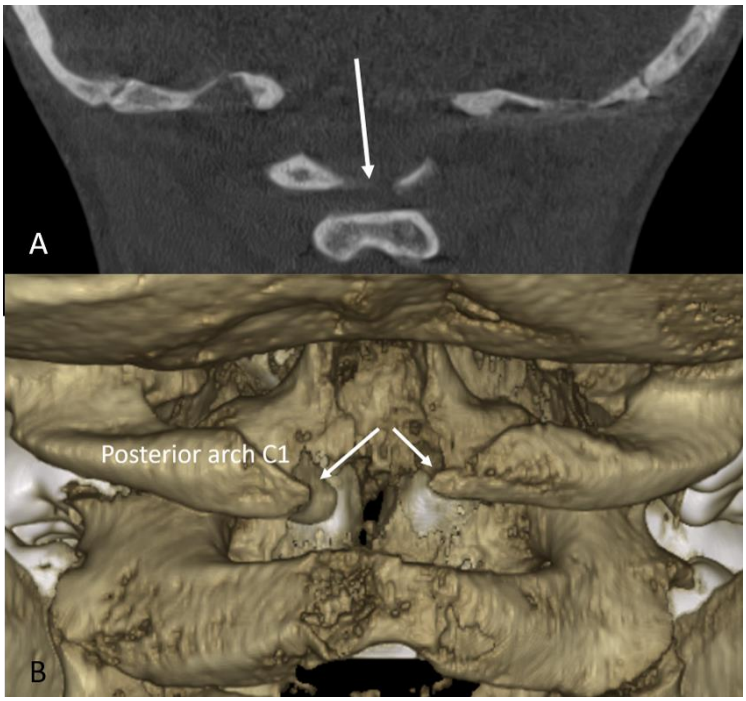

Fig. 45. Coronal view. Arrow: absence of the fusion of the posterior arch on the midline. B. 3D reconstruction. Posterior view of the C1 vertebra. Arrows: absence of the fusion of the posterior arch on the midline. Dehiscence between both posterior arches.

Step 6. 3D soft tissue reconstruction: we search for external ear anomalies. We found no anomalies of external ears in this patient.

There were no anomalies of external ears for this patient.

Discussion

In 2014 Miles et al. stated that 98% radiologists do not learn how to report information from CBCT volume [64]. Therefore, Miles et al proposed their own system or reporting CBCT data in head and neck area to help radiologists communicate with other specialities [64]. Similar system was further proposed by Kachlan et al. [65]. However, these systems were not supposed to be used in pediatric nor in CLP patients CBCT examinations. Reporting systems by Miles and Kachlan needed the use of CBCT with large field of view incorporating areas from the skull, through orbits to the neck area (Table 1). Santos et al., proposed a system of reporting

incidental findings on CBCT of CLP patients using most of items of the Miles's methodology [66]. Santos added the reporting of information from the mandible, from the orbit, and from the middle and inner ear cavity [66]. Again, a large field of view is needed to report information from all of these areas. We choose to avoid the mandible and the orbit in the selected field of view as most indications of use of the CBCT in CLP patients are related to the maxilla [1-7]. We do not use "Gap" in Gand classification as this classification of the missing alveolar bone area is too simplified and subjective (Table 1) [17]. We do not use either "Arch" GAND classification which corresponds to the discrimination between anterior and posterior endognathia of the maxilla (Table 1) [17]. We do not use "Nasal" transversal GAND classification as we describe the sagittal anteroposterior extension of the cleft palate (Table 1) [17]. We do not use "Dental" GAND global classification as we describe tooth by tooth along the dental arch from right to left (Table 1) [17]. The dental classification by Bezerra et al., is only limited to the central and lateral incisors (Table 1) [67]. We describe also the 3D position of all of the teeth on the dental arch starting from posterior to anterior, and using the six degree of freedom reference frame (3 translations and 3 rotations) [56]. As Santos et al., we systematically describe the upper cervical spine [66], the atlas and the axis vertebra [58]. We are also using the natural contrast between the air and external soft tissue to evaluate the modifications in the shape of external ears that may occur in CLP syndromic patients. Moreover, we suggest the type of image modality such as axial, coronal, sagittal 2D view or 3D reconstruction which may be suited for a specific purpose. We provide with 46 freely accessible figures in contrast with only 3 available open-access figures from literature [67].

Table 1. Modes of reporting information from CBCT volume.

Modes of reporting	Literature methodologies	Our methodology
General approach		
Miles et al (2014) [64]	1) Paranasal sinuses, 2) Nasal cavity, 3) Airway, 4) Cervical structures, 5) TMJs, 6) Dental findings, 7) Other findings	Include: Paranasal sinuses, nasal cavity, cervical structures, dental findings Exclude: airway, TMJ
Kachlan et al (2021) [65]	1) Jaws, 2) Paranasal sinus, 3) Nasal fossa, 4) Pharyngeal airway, 5) Neck soft tissues, 6) TMJ, 7) Skull base/brain, and 8) Others	
Cleft palate general description		
Santos et al (2020) [66]	1) Paranasal sinuses, 2) Pharynx (airway), 3) Cervical spine, 4) TMJ, 5) Maxilla, and 6) Mandible, and 7) Abnormal teeth*, 8) Orbit, 9) Middle and inner ear cavity,	Include: paranasal sinuses, cervical spine, maxilla, skull Exclude: airway, mandible, orbit, middle and inner ear cavity

	10) Skull	*Not limited to the description of only abnormal teeth
Barbosa et al (2016) [17] GAND classification		
	Gap: notch, small, large size of the gap	Not used
	Arch: aligned, anterior constriction, anterior and posterior constriction	Not used
	Nasal: nasal floor: (cleft palate): notch, small, large	More descriptive approach (complete, partial cleft palate, anterior, posterior, fistula)
	Dental: normal, supernumerary/malformed, missing	Full description of all maxillary teeth
Bezerra et al (2017) [67] Tooth development in CLP patients		
	Agenesis (second incisor, second premolar)	Not limited to this category only
	Microdontia (conical lateral incisor)	Not limited to this category only
	Giroversion (central incisor)	Not limited to this category only

We are using large field of view (16x6.2cm) which may contain temporal bone. The international recommendations from 2011 insist on the dentist responsibility of reporting on the entire field of view [63]. Therefore, future development of our methodology should contain the systematic exploration of the middle and inner ear cavity (Figure 46) [66].

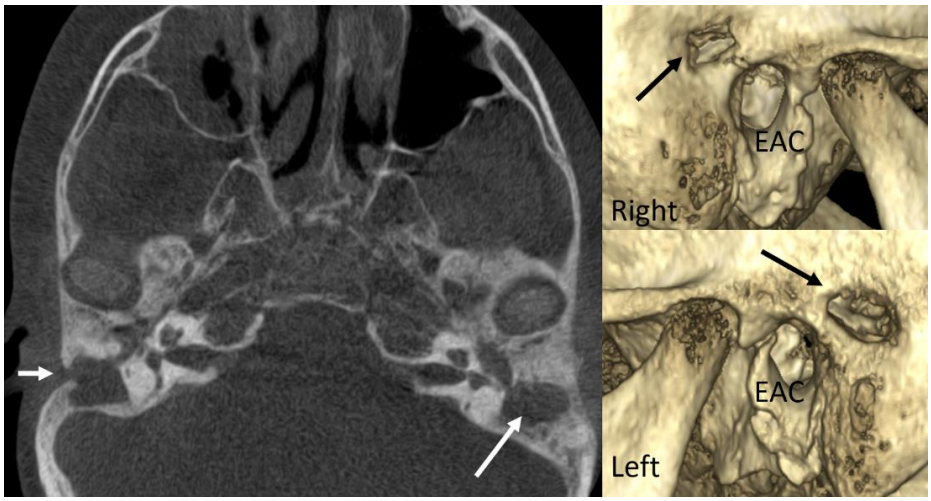

Fig. 46. Planmeca Promax 3D Mid. Patient 10 years-old. Axial view. Arrows: traces of temporal bone surgery. 3D reconstruction. Right view: arrow: surgical perforation of the right temporal bone in posterior and apical to the right external auditory canal (EAC). Left side: arrow: surgical perforation of the left temporal bone in apical to the left external auditory canal.

- **Acknowledgements**: this study was presented at the Charity MedCongress for Ukraine army veterans, Lviv, Ukraine, 3.12.2022.
- **Funding sources statement**: this study does not receive any funding
- **Competing interests**: Prof R. Olszewski is Editor-in-Chief of Nemesis. The other authors declare no conflict of interest.
- **Ethical approval**: We obtained the approval from our University and Hospital Ethical committee for this study (B403/2019/03DEC/542)
- **Informed consent**: Patients were exempted from the informed consent according to the ethical committee approval.

Authors contribution:

Author	Contributor role
Olszewski Raphael	Conceptualization, Investigation, Methodology, Data curation, Resources, Validation, Writing original draft preparation, Supervision, Writing review and editing
De Muylder Antoine	Data curation, Writing review and editing
Siciliano Sergio	Data curation, Writing review and editing

References

1. Gümrü B, Guldali M, Tarcin B, Idman E, Sertac Peker M. Evaluation of cone beam computed tomography referral profile: Retrospective study in a Turkish paediatric subpopulation. Eur J Paediatr Dent 2021;22:66-70. https://doi.org/10.23804/ejpd.2021.22.01.12.

2. Theys S, Olszewski R. Cone beam computed tomography (CBCT) in pediatric dentistry. Nemesis 2022;25:1-43. https://doi.org/10.14428/nemesis.v25i1.

3. Kuijpers MA, Chiu YT, Nada RM, Carels CE, Fudalej PS. Three-dimensional imaging methods for quantitative analysis of facial soft tissues and skeletal morphology in patients with orofacial clefts: a systematic review. PLoS One 2014;9:e93442. https://doi.org/10.1371/journal.pone.0093442.

4. Kuijpers-Jagtman AM, Kuijpers MAR, Schols GJH, Maal TJJ, Breuning KH, van Vlijmen OJC. The use of cone-beam computed tomography for orthodontic purposes. Seminars Orthod 2013;19:196-203.

5. Coşkun İ, Kaya B. Cone beam computed tomography in orthodontics. Turk J Orthod 2018;31: 55–61. https://doi.org/10.5152/TurkJOrthod.2018.18020.

6. De Grauwe A, Ayaz I, Shujaat S, Dimitrov S, Gbadegbegnon L, Vande Vannet B, Jacobs R. CBCT in orthodontics: a systematic review on justification of CBCT in a paediatric population prior to orthodontic treatment. Eur J Orthod 2019;41:381-389. https://doi.org/10.1093/ejo/cjy066.

7. Kapila SD, Nervina JM. CBCT in orthodontics: assessment of treatment outcomes and indications for its use. Dentomaxillofac Radiol 2015;44:20140282. https://doi.org/10.1259/dmfr.20140282.

8. Etemadi Sh M, Movahedian Attar B, Mehdizadeh M, Tajmiri G. Evaluation of the CBCT imaging accuracy in the volumetric assessment of unilateral alveolar cleft. J Stomatol Oral Maxillofac Surg 2021;122:e1-e5. https://doi.org/10.1016/j.jormas.2021.06.006.

9. Janssen NG, Schreurs R, Bittermann GKP, Borstlap WA, Koole R, Meijer GJ, Maal TJJ. A novel semi-automatic segmentation protocol for volumetric assessment of alveolar cleft grafting procedures. J Craniomaxillofac Surg 2017;45:685-689. https://doi.org/10.1016/j.jcms.2017.02.018.

10. Zhou WN, Xu YB, Jiang HB, Wan L, Du YF. Accurate evaluation of cone-beam computed tomography to volumetrically assess bone grafting in alveolar cleft patients. J Craniofac Surg 2015;26:e535-e539. https://doi.org/10.1097/SCS.0000000000002034.

11. Dissaux C, Bodin F, Grollemund B, Bridonneau T, Kauffmann I, Mattern JF, Bruant-Rodier C. Evaluation of success of alveolar cleft bone graft performed at 5 years versus 10 years of age. J Craniomaxillofac Surg 2016;44:21-26. https://doi.org/10.1016/j.jcms.2015.09.003.

12. Chen PR, Lin YC, Pai BC, Tseng HJ, Lo LJ, Chou PY. Progressive comparison of density assessment of alveolar bone graft in patients with unilateral and bilateral cleft. J Clin Med 2021;10:5143. https://doi.org/10.3390/jcm10215143.

13. Linderup BW, Cattaneo PM, Jensen J, Küseler A. Mandibular symphyseal bone graft for reconstruction of alveolar cleft defects: Volumetric assessment with cone beam computed tomography 1-year postsurgery. Cleft Palate Craniofac J 2016;53:64-72. https://doi.org/10.1597/14-143.

14. Kochhar AS, Sidhu MS, Prabhakar M, Bhasin R, Kochhar GK, Dadlani H, Spagnuolo G, Mehta VV. Intra- and interobserver reliability of bone volume estimation using OsiriX software in patients with cleft lip and palate using cone beam computed tomography. Dent J (Basel) 2021;9:14. https://doi.org/10.3390/dj9020014.

15. Datana S, Chattopadhyay PK, Kadu A. Bony bridge resorption after secondary alveolar grafting and correlation with success of orthodontic treatment: A prospective volumetric cone beam computed tomography (CBCT) study. Med J Armed Forces India 2019;75:375-382. https://doi.org/10.1016/j.mjafi.2018.02.005.

16. Suomalainen A, Åberg T, Rautio J, Hurmerinta K. Cone beam computed tomography in the assessment of alveolar bone grafting in children with unilateral cleft lip and palate. Eur J Orthod 2014;36:603-611. https://doi.org/10.1093/ejo/cjt105.

17. Barbosa GL, Emodi O, Pretti H, van Aalst JA, de Almeida SM, Tyndall DA, Pimenta LA. GAND classification and volumetric assessment of unilateral cleft lip and palate malformations using cone beam computed tomography. Int J Oral Maxillofac Surg 2016;45:1333-1340. https://doi.org/10.1016/j.ijom.2016.05.008.

18. Attar BM, Soltani P, Davari D, Mehdizadeh M. Cone-beam computed tomographic comparison of chin symphysis bone particles and allograft versus iliac crest bone graft alone for reconstruction of alveolar bone defects in cleft patients. J Korean Assoc Oral Maxillofac Surg 2022;48:85-93. https://doi.org/10.5125/jkaoms.2022.48.2.85.

19. Padwa BL, Tio P, Garkhail P, Nuzzi LC. Cone beam computed tomographic analysis demonstrates a 94% radiographic success rate in 783 alveolar bone grafts. J Oral Maxillofac Surg 2022;80:633-640. https://doi.org/10.1016/j.joms.2021.12.004.

20. Gu Y, Yan C, Yan Z, Wang X, Yue L, Li L. Evaluation of the clinical efficacy and safety of modified alveolar cleft bone graft with cone-beam CT digital imaging in children. Transl Pediatr 2022;11:1140-1148. https://doi.org/10.21037/tp-22-214.

21. Oberoi S, Gill P, Chigurupati R, Hoffman WY, Hatcher DC, Vargervik K. Three-dimensional assessment of the eruption path of the canine in individuals with bone-grafted alveolar clefts using cone beam computed tomography. Cleft Palate Craniofac J 2010;47:507-512. https://doi.org/10.1597/08-171.

22. Touzet-Roumazeille S, Vi-Fane B, Kadlub N, Genin M, Dissaux C, Raoul G, Ferri J, Vazquez MP, Picard A. Osseous and dental outcomes of primary gingivoperiosteoplasty with iliac bone graft: A radiological evaluation. J Cranio-maxillofac Surg 2015;43:950-955. https://doi.org/10.1016/j.jcms.2015.03.027.

23. Linderup BW, Küseler A, Jensen J, Cattaneo PM. A novel semiautomatic technique for volumetric assessment of the alveolar bone defect using cone beam computed tomography. Cleft Palate Craniofac J 2015;52:e47-55. https://doi.org/10.1597/13-287.

24. Garib DG, Yatabe MS, Ozawa TO, Filho OG. Alveolar bone morphology in patients with bilateral complete cleft lip and palate in the mixed dentition: cone beam computed tomography evaluation. Cleft Palate Craniofac J 2012;49:208-214. https://doi.org/10.1597/10-198.

25. Girinon F, Ketoff S, Hennocq Q, Kogane N, Ullman N, Kadlub N, Galliani E, Neiva-Vaz C, Vazquez MP, Picard A, Khonsari RH. Maxillary shape after primary cleft closure and before alveolar bone graft in two different management protocols: A comparative morphometric study. J Stomatol Oral Maxillofac Surg 2019;120:406-409. https://doi.org/10.1016/j.jormas.2019.02.001.

26. Hechler SL. Cone-beam CT: applications in orthodontics. Dent Clin North Am 2008;52:809-823. https://doi.org/10.1016/j.cden.2008.05.001.

27. Tadinada A, Schneider S, Yadav S. Role of cone beam computed tomography in contemporary orthodontics. Semin Orthod 2018;24:407-415. https://doi.org/10.1053/j.sodo.2018.10.005.

28. Nervina JM. Cone beam computed tomography use in orthodontics. Austral Dent J 2012;57:95-102. https://doi.org/10.1111/j.1834-7819.2011.01662.x.

29. Parveen S, Husain A, Mascarenhas R, Reddy SG. Clinical utility of cone-beam computed tomography in patients with cleft lip palate: Current perspectives and guidelines. J Cleft Lip Palate Craniofac Anomal 2018;5:74-87. https://doi.org/10.4103/jclpca.jclpca_7_18.

30. Singh S, Batra P, Raghavan S, Sharma K, Srivastava A. Evaluation of Alt-RAMEC with facemask in patients with unilateral cleft lip and palate (UCLP) using cone beam computed tomography (CBCT) and finite element modeling-A clinical

prospective study. Cleft Palate Craniofac J. 2022;59:166-176. https://doi.org/10.1177/10556656211000968.

31. de Almeida AM, Ozawa TO, Alves ACM, Janson G, Lauris JRP, Ioshida MSY, Garib DG. Slow versus rapid maxillary expansion in bilateral cleft lip and palate: a CBCT randomized clinical trial. Clin Oral Investig 2017;21:1789-1799. https://doi.org/10.1007/s00784-016-1943-8.

32. Steegman RM, Klein Meulekamp AF, Dieters A, Jansma J, van der Meer WJ, Ren Y. Skeletal changes in growing cleft patients with class III malocclusion treated with bone anchored maxillary protraction-A 3.5-year follow-up. J Clin Med 2021;10:750. https://doi.org/10.3390/jcm10040750.

33. Ren Y, Steegman R, Dieters A, Jansma J, Stamatakis H. Bone-anchored maxillary protraction in patients with unilateral complete cleft lip and palate and Class III malocclusion. Clin Oral Investig 2019;23:2429-2441. https://doi.org/10.1007/s00784-018-2627-3.

34. Alrejaye N, Gao J, Hatcher D, Oberoi S. Effect of maxillary expansion and protraction on the oropharyngeal airway in individuals with non-syndromic cleft palate with or without cleft lip. PLoS One 2019;14:e0213328. https://doi.org/10.1371/journal.pone.0213328.

35. Stangherlin Gomes O, Carvalho RM, Faco R, Yatabe M, Ozawa TO, De Clerck H, Timmerman H, Garib D. Influence of bone-anchored maxillary protraction on secondary alveolar bone graft status in unilateral complete cleft lip and palate. Am J Orthod Dentofacial Orthop 2020;158:731-737. https://doi.org/10.1016/j.ajodo.2019.10.021.

36. Garib D, Miranda F, Sathler R, Kuijpers-Jagtman AM, Aiello CA. Rapid maxillary expansion after alveolar bone grafting with rhBMP-2 in UCLP evaluated by means of CBCT. Cleft Palate Craniofac J 2017;54:474-480. https://doi.org/10.1597/15-133.

37. Parveen S, Husain A, Johns G, Mascarenhas R, Reddy SG. Three-dimensional analysis of craniofacial structures of individuals with nonsyndromic unilateral complete cleft lip and palate. J Craniofac Surg 2021;32:e65-e69. https://doi.org/10.1097/SCS.0000000000006933.

38. Yang L, Chen Z, Zhang X. A cone-beam computed tomography evaluation of facial asymmetry in unilateral cleft lip and palate individuals. J Oral Sci 2016;58:109-115. https://doi.org/10.2334/josnusd.58.109.

39. Lin Y, Chen G, Fu Z, Ma L, Li W. Cone-beam computed tomography assessment of lower facial asymmetry in unilateral cleft lip and palate and non-cleft

patients with class III skeletal relationship. PLoS One 2015;10:e0130235. https://doi.org/10.1371/journal.pone.0130235.

40. Shrestha A, Takahashi M, Yamaguchi T, Adel M, Furuhata M, Hikita Y, Yoshida H, Nakawaki T, Maki K. Three-dimensional evaluation of mandibular volume in patients with cleft lip and palate during the deciduous dentition period. Angle Orthod 2020;90:85-91. https://doi.org/10.2319/112618-831.1.

41. Yatabe M, Garib D, Faco R, de Clerck H, Souki B, Janson G, Nguyen T, Cevidanes L, Ruellas A. Mandibular and glenoid fossa changes after bone-anchored maxillary protraction therapy in patients with UCLP: A 3-D preliminary assessment. Angle Orthod 2017;87:423-431. https://doi.org/10.2319/052516-419.1.

42. Akay G, Eren I, Karadag O, Gungor K. Three-dimensional assessment of the sella turcica: comparison between cleft lip and palate patients and skeletal malocclusion classes. Surg Radiol Anat 2020;42:977-983. https://doi.org/10.1007/s00276-020-02481-z.

43. Kiaee B, Nucci L, Sarkarat F, Talaeipour AR, Eslami S, Amiri F, Jamilian A. Three-dimensional assessment of airway volumes in patients with unilateral cleft lip and palate. Prog Orthod. 2021;22:35. https://doi.org/10.1186/s40510-021-00382-4.

44. Pimenta LA, de Rezende Barbosa GL, Pretti H, Emodi O, van Aalst J, Rossouw PE, Tyndall DA, Drake AF. Three-dimensional evaluation of nasopharyngeal airways of unilateral cleft lip and palate patients. Laryngoscope 2015;125:736-739. https://doi.org/10.1002/lary.24895.

45. Cheung T, Oberoi S. Three dimensional assessment of the pharyngeal airway in individuals with non-syndromic cleft lip and palate. PLoS One 2012;7:e43405. https://doi.org/10.1371/journal.pone.0043405.

46. Takahashi M, Yamaguchi T, Lee MK, Suzuki Y, Adel M, Tomita D, Nakawaki T, Yoshida H, Hikita Y, Furuhata M, Tsuneoka M, Nagahama R, Marazita ML, Weinberg SM, Maki K. Three-dimensional assessment of the pharyngeal airway in Japanese preschoolers with orofacial clefts. Laryngoscope 2020;130:533-540. https://doi.org/10.1002/lary.27957.

47. Iwasaki T, Suga H, Minami-Yanagisawa A, Hashiguchi-Sato M, Sato H, Yamamoto Y, Shirazawa Y, Tsujii T, Kanomi R, Yamasaki Y. Upper airway in children with unilateral cleft lip and palate evaluated with computational fluid dynamics. Am J Orthod Dentofacial Orthop 2019;156:257-265. https://doi.org/10.1016/j.ajodo.2018.09.013.

48. Al-Fahdawi MA, El-Kassaby MA, Farid MM, El-Fotouh MA. Cone beam computed tomography analysis of oropharyngeal airway in preadolescent nonsyndromic

bilateral and unilateral cleft lip and palate patients. Cleft Palate Craniofac J 2018;55:883-890. https://doi.org/10.1597/15-322.

49. Ko J, Han HJ, Hoffman W, Oberoi S. Three-dimensional analysis of cortical bone thickness in individuals with non-syndromic unilateral cleft lip and palate. J Craniofac Surg 2019;30:2094-2098. https://doi.org/10.1097/SCS.0000000000005988.

50. Moscarino S, Scholz J, Bastian A, Knaup I, Wolf M. Bone and soft tissue palatal morphology and potential anchorage sides in cleft palate patients. Ann Anat 2019;224:41-46. https://doi.org/10.1016/j.aanat.2019.02.005.

51. Kang BC, Yoon SJ, Lee JS, Al-Rawi W, Palomo JM. The use of cone beam computed tomography for the evaluation of pathology, developmental anomalies and traumatic injuries relevant to orthodontics. Semin Orthod 2011;17:20-33. https://doi.org/10.1053/j.sodo.2010.08.005.

52. Lopes de Rezende Barbosa G, Pimenta LA, Pretti H, Golden BA, Roberts J, Drake AF. Difference in maxillary sinus volumes of patients with cleft lip and palate. Int J Pediatr Otorhinolaryngol 2014;78:2234-2236. https://doi.org/10.1016/j.ijporl.2014.10.019.

53. Wang X, Zhang M, Han J, Wang H, Li S.Three-dimensional evaluation of maxillary sinus and maxilla for adolescent patients with unilateral cleft lip and palate using cone-beam computed tomography. Int J Pediatr Otorhinolaryngol 2020;135:110085. https://doi.org/10.1016/j.ijporl.2020.110085.

54. Li J, Shi B, Liu K, Zheng Q. A preliminary study on the hard-soft tissue relationships among unoperated secondary unilateral cleft nose deformities. Oral Surg Oral Med Oral Pathol Oral Radiol 2012;113:300-307. https://doi.org/10.1016/j.tripleo.2011.03.007.

55. Massie JP, Bruckman K, Rifkin WJ, Runyan CM, Shetye PR, Grayson B, Flores RL. The effect of nasoalveolar molding on nasal airway anatomy: A 9-year follow-up of patients with unilateral cleft lip and palate. Cleft Palate Craniofac J 2018;55:596-601. https://doi.org/10.1177/1055665617744062.

56. Alqahtani K, Shaheen E, Shujaat S, EzEldeen M, Dormaar T, de Llano-Pérula MC, Politis C, Jacobs R. Validation of a novel method for canine eruption assessment in unilateral cleft lip and palate patients. Clin Exp Dent Res 2021;7:285-292. https://doi.org/10.1002/cre2.397.

57. Sandhu SK. Cone beam computed tomography in orthodontics. Saint's Int Dent J 2017;3:1-3. https://doi.org/10.4103/sidj.sidj_1_18.

58. Berrocal C, Terrero-Pérez A, Peralta-Mamani M, Fischer Rubira-Bullen IR, Marques Honorio H, Marchi de Carvalho IM, Alvares Capelozza AL. Cervical vertebrae anomalies and cleft lip and palate: a systematic review and meta-analysis. Dentomaxillofac Radiol 2019;48: 20190085. https://doi.org/10.1259/dmfr.20190085.

59. Patel S, Harvey S. Guidelines for reporting on CBCT scans. Int Endod J 2021;54:628-633. https://doi.org/10.1111/iej.13443.

60. Kim IH, Singer SR, Mupparapu M. Review of cone beam computed tomography guidelines in North America. Quintessence Int 2019;50:136-145. https://doi.org/10.3290/j.qi.a41332.

61. Harvey S, Patel S. Guidelines and template for reporting on CBCT scans. Br Dent J 2020;228:15-18. https://doi.org/10.1038/s41415-019-1115-8.

62. Noar JH, Pabari S. Cone beam computed tomography--current understanding and evidence for its orthodontic applications? J Orthod 2013;40:5-13. https://doi.org/10.1179/1465313312Y.0000000040.

63. Scarfe WC, Li Z, Aboelmaaty W, Scott SA, Farman AG. Maxillofacial cone beam computed tomography: essence, elements and steps to interpretation. Aust Dent J 2012;57:46-60. https://doi.org/10.1111/j.1834-7819.2011.01657.x.

64. Miles DA, Danforth RA. Reporting findings in the cone beam computed tomography volume. Dent Clin North Am 2014;58:687-709. https://doi.org/10.1016/j.cden.2014.04.006.

65. Kachlan MO, Yang J, Balshi TJ, Wolfinger GJ, Balshi SF. Incidental findings in cone beam computed tomography for dental implants in 1002 patients. J Prosthodont 2021;30:665-675. https://doi.org/10.1111/jopr.13329.

66. Santos G, Ickow I, Job J, Brooker JE, Dvoracek LA, Rigby E, Shah N, Chen W, Branstetter B, Schuster LA. Cone-beam computed tomography incidental findings in individuals with cleft lip and palate. Cleft Palate Craniofac J 2020;57:404-411. https://doi.org/10.1177/1055665619897469.

67. Bezerra BT, Pinho JN, da Silva LC. Tooth abnormalities in individuals with unilateral alveolar clefts: A comparison between sides using cone-beam computed tomography. J Clin Exp Dent 2017;9:e1195-e1200. https://doi.org/10.4317/jced.54043.